

REPORT DOCUMENTATION PAGE				Form Approved OMB No. 0704-0188	
Public reporting burden for this collection of information is estimated to average 1 hour per response, including the time for reviewing instructions, searching existing data sources, gathering and maintaining the data needed, and completing and reviewing this collection of information. Send comments regarding this burden estimate or any other aspect of this collection of information, including suggestions for reducing this burden to Department of Defense, Washington Headquarters Services, Directorate for Information Operations and Reports (0704-0188), 1215 Jefferson Davis Highway, Suite 1204, Arlington, VA 22202-4302. Respondents should be aware that notwithstanding any other provision of law, no person shall be subject to any penalty for failing to comply with a collection of information if it does not display a currently valid OMB control number. <b>PLEASE DO NOT RETURN YOUR FORM TO THE ABOVE ADDRESS.</b>					
1. REPORT DATE (DD-MM-YYYY) 20-03-2006		2. REPORT TYPE Journal Article		3. DATES COVERED (From - To)	
4. TITLE AND SUBTITLE  <b>Experimental Evidence for Linear Metal-Azide Bonds. The Binary Group 5 Azides (Nb(N<sub>3</sub>)<sub>5</sub>, Ta(N<sub>3</sub>)<sub>5</sub>, [Nb(N<sub>3</sub>)<sub>6</sub>]<sup>-</sup> and [Ta(N<sub>3</sub>)<sub>6</sub>]<sup>-</sup>, and 1:1 Adducts of Nb(N<sub>3</sub>)<sub>5</sub> and Ta(N<sub>3</sub>)<sub>5</sub> with CH<sub>3</sub>CN (PREPRINT)</b>				5a. CONTRACT NUMBER	
				5b. GRANT NUMBER	
				5c. PROGRAM ELEMENT NUMBER	
6. AUTHOR(S) Ralf Haiges, Thorsten Schroer, Muhammed Yousufuddin, & Karl Christe (USC); Jerry A. Boatz (AFRL/PRSP)				5d. PROJECT NUMBER	
				5e. TASK NUMBER 23030423	
				5f. WORK UNIT NUMBER	
7. PERFORMING ORGANIZATION NAME(S) AND ADDRESS(ES)  Air Force Research Laboratory (AFMC) AFRL/PRSP 10 E. Saturn Blvd. Edwards AFB CA 93524-7680				8. PERFORMING ORGANIZATION REPORT NUMBER  AFRL-PR-ED-JA-2006-103	
9. SPONSORING / MONITORING AGENCY NAME(S) AND ADDRESS(ES)  Air Force Research Laboratory (AFMC) AFRL/PRS 5 Pollux Drive Edwards AFB CA 93524-7048				10. SPONSOR/MONITOR'S ACRONYM(S)	
				11. SPONSOR/MONITOR'S NUMBER(S) AFRL-PR-ED-JA-2006-103	
12. DISTRIBUTION / AVAILABILITY STATEMENT  Approved for public release; distribution unlimited (AFRL-ERS-PAS-2006-085)					
13. SUPPLEMENTARY NOTES Submitted to Angewandte Chemie.					
14. ABSTRACT  Whereas the existence of numerous binary transition metal azido-complexes has been reported, <sup>[1-3]</sup> no binary Group 5 azides are known. Only a limited number of partially azide-substituted compounds of vanadium, niobium and tantalum have previously been reported. <sup>[4-21]</sup> In this paper, we wish to communicate the synthesis and characterization of Nb(N <sub>3</sub> ) <sub>5</sub> , Ta(N <sub>3</sub> ) <sub>5</sub> and their 1:1 adducts with CH <sub>3</sub> CN, and of the anions [Nb(N <sub>3</sub> ) <sub>6</sub> ] <sup>-</sup> and [Ta(N <sub>3</sub> ) <sub>6</sub> ] <sup>-</sup> . The crystal structures of Nb(N <sub>3</sub> ) <sub>5</sub> ·CH <sub>3</sub> CN and [PPh <sub>4</sub> ][Nb(N <sub>3</sub> ) <sub>6</sub> ] <sup>-</sup> and the first experimental evidence for the existence of azido compounds with linear metal-N-N bonds are also reported.					
15. SUBJECT TERMS					
16. SECURITY CLASSIFICATION OF:			17. LIMITATION OF ABSTRACT  A	18. NUMBER OF PAGES  37	19a. NAME OF RESPONSIBLE PERSON Dr. Scott A. Shackelford
a. REPORT  Unclassified	b. ABSTRACT  Unclassified	c. THIS PAGE  Unclassified			19b. TELEPHONE NUMBER (include area code) N/A

# Experimental Evidence for Linear Metal-Azide Bonds. The Binary Group 5 Azides $\text{Nb}(\text{N}_3)_5$ , $\text{Ta}(\text{N}_3)_5$ , $[\text{Nb}(\text{N}_3)_6]^-$ and $[\text{Ta}(\text{N}_3)_6]^-$ , and 1:1 Adducts of $\text{Nb}(\text{N}_3)_5$ and $\text{Ta}(\text{N}_3)_5$ with $\text{CH}_3\text{CN}$ \*\* (Preprint)

Ralf Haiges<sup>\*</sup>, Jerry A. Boatz, Thorsten Schroer, Muhammed Yousufuddin, and Karl O. Christe<sup>\*</sup>

*Dedicated to Professor Reint Eujen on the occasion of his 60th birthday*

Whereas the existence of numerous binary transition metal azido-complexes has been reported,<sup>[1-3]</sup> no binary Group 5 azides are known. Only a limited number of partially azide-substituted compounds of vanadium, niobium and tantalum have previously been reported.<sup>[4-21]</sup>

In this paper, we wish to communicate the synthesis and characterization of  $\text{Nb}(\text{N}_3)_5$ ,  $\text{Ta}(\text{N}_3)_5$  and their 1:1 adducts with  $\text{CH}_3\text{CN}$ , and of the anions  $[\text{Nb}(\text{N}_3)_6]^-$  and  $[\text{Ta}(\text{N}_3)_6]^-$ . The crystal structures of  $\text{Nb}(\text{N}_3)_5 \cdot \text{CH}_3\text{CN}$  and  $[\text{PPh}_4][\text{Nb}(\text{N}_3)_6]$  and the first experimental evidence for the existence of azido compounds with linear metal-N-N bonds are also reported.

The reactions of  $\text{NbF}_5$  or  $\text{TaF}_5$  with excess  $(\text{CH}_3)_3\text{SiN}_3$  in  $\text{SO}_2$  solution at  $-20^\circ\text{C}$  result in

---

[\*] Dr. R. Haiges, Dr. T. Schroer, Dr. M. Yousufuddin, Prof. Dr. K. O. Christe

Loker Research Institute and Department of Chemistry

University of Southern California

Los Angeles, CA 90089-1661 (USA)

Fax: (+1) 213-740-6679

E-mail: [haiges@usc.edu](mailto:haiges@usc.edu), [kchriste@usc.edu](mailto:kchriste@usc.edu)

Dr. J. A. Boatz

Space and Missile Propulsion Division

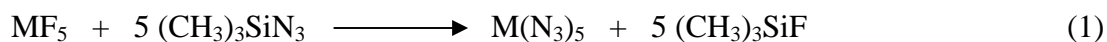
Air Force Research Laboratory (AFRL/PRSP)

10 East Saturn Boulevard, Bldg 8451

Edwards Air Force Base, CA 93524 (USA)

[\*\*] This work was funded by the Air Force Office of Scientific Research and the National Science Foundation. We thank Prof. Dr. G. A. Olah, and Dr. M. Berman, for their steady support, and Prof. D. Dixon, Prof. Dr. R. Bau, Drs. R. Wagner and W. W. Wilson, and C. Bigler Jones for their help and stimulating discussions. We gratefully acknowledge grants of computer time at the Aeronautical Systems Center (Wright-Patterson Air Force Base, Dayton, OH), the Naval Oceanographic Office (Stennis Space Center, MS), the Engineer Research and Development Center (Vicksburg, MS), the Army Research Laboratory (Aberdeen Proving Ground, MD), and the Army High Performance Computing Research Center (Minneapolis, MN), under sponsorship of the Department of Defense High Performance Computing Modernization Program Office.

complete fluoride-azide exchange and yield clear solutions of Nb(N<sub>3</sub>)<sub>5</sub> or Ta(N<sub>3</sub>)<sub>5</sub>, respectively, [Eq. (1) (M = Nb, Ta)].



When the volatile compounds, SO<sub>2</sub>, (CH<sub>3</sub>)<sub>3</sub>SiF and excess (CH<sub>3</sub>)<sub>3</sub>SiN<sub>3</sub>, are pumped off at -20 °C, pure, yellow, solid, room-temperature stable pentaazides are produced in quantitative yield. As expected for covalently bonded polyazides,<sup>[22]</sup> they are shock sensitive and can explode violently when touched with a metal spatula or by heating in the flame of a Bunsen burner. Their identity was established by the observed mass-balances, vibrational spectroscopy and their conversions with N<sub>3</sub><sup>-</sup> into hexaazido-metalates and with CH<sub>3</sub>CN into 1:1 acetonitrile donor-acceptor adducts, as shown by the crystal structures of [P(C<sub>6</sub>H<sub>5</sub>)<sub>4</sub>]<sup>+</sup>[Nb(N<sub>3</sub>)<sub>6</sub>]<sup>-</sup> and Nb(N<sub>3</sub>)<sub>5</sub>·CH<sub>3</sub>CN.

The observed infrared and Raman spectra of Nb(N<sub>3</sub>)<sub>5</sub> and Ta(N<sub>3</sub>)<sub>5</sub> are shown in Figures S1 and S2, respectively, of the Supplementary Material, and the observed frequencies and intensities are listed in the Experimental Section. They were assigned (see Tables S1 and S2 of the Supplementary Material) by comparison with those calculated at the B3LYP<sup>[23]</sup> and MP2<sup>[24]</sup> levels of theory using SBKJ-(d) basis sets.<sup>[25]</sup> The agreement between observed and calculated spectra is satisfactory and supports trigonal-bipyramidal structures (Table 1) for Nb(N<sub>3</sub>)<sub>5</sub> and Ta(N<sub>3</sub>)<sub>5</sub>. The internal modes of the azido ligands are split into clusters of five due to in-phase and out-of-phase coupling of the individual motions. There are always one in-phase and four out-of-phase vibrations, with the in-phase one readily identifiable from its higher Raman intensity. The MN<sub>5</sub> skeletal modes can be derived from *D*<sub>3h</sub> symmetry in which the double degeneracy of the E modes is lifted due to the presence of the azido ligands which lowers the overall symmetry to *C*<sub>s</sub> and is likely to produce some distortion from *D*<sub>3h</sub>.

Whereas trigonal-bipyramidal arrangements of the azido ligands have previously also been found for  $[\text{Fe}(\text{N}_3)_5]^{2-}$ ,<sup>[26]</sup> and theoretically predicted for  $\text{Sb}(\text{N}_3)_5$  and  $\text{As}(\text{N}_3)_5$ ,<sup>[27,28]</sup> the details of these structures are very different. In  $[\text{Fe}(\text{N}_3)_5]^{2-}$ ,  $\text{As}(\text{N}_3)_5$  and  $\text{Sb}(\text{N}_3)_5$ , all five M-N-N bonds are strongly bent, and the two axial M-N bonds are significantly longer than the equatorial ones, as expected from VSEPR arguments.<sup>[29]</sup> In contrast, the axial M-N-N bonds in  $\text{Nb}(\text{N}_3)_5$  and  $\text{Ta}(\text{N}_3)_5$  are calculated to be almost linear, while the equatorial ones have angles of about 137 °. Furthermore, all five M-N bonds and the internal N-N distances of the five azido ligands are essentially the same.

Linear M-N-N bonds had previously been predicted also for the tetraazides of  $d^0$  Ti(+IV), Zr(+IV), and Hf(+IV)<sup>[30]</sup> and for  $d^6$  Fe(+II),<sup>[31]</sup> but the hexazido dianion of  $d^0$  Ti(+IV) was shown experimentally to possess strongly bent Ti-N-N bonds.<sup>[1]</sup> These findings show that the linearity of the M-N-N bonds cannot be caused by either a trigonal-bipyramidal structure, multiple M-N bonds, or a  $d^0$  electronic configuration *per se*.

The occurrence of linear metal-N-N groups can be predicted by theoretical calculations.<sup>[30,31]</sup> A plausible explanation for the linearity of these M-N-N bonds has recently been given,<sup>[1]</sup> based on an analogy with the known crystal structure of  $\text{Zr}(\text{BH}_4)_4$ .<sup>[32]</sup> A model was proposed in which the  $\text{N}_\alpha$  atom of the azides acts as a tridative ligand. A detailed analysis of the occurrence of linear M-N-N bonds in the periodic system and of the nature of these bonds is presently being carried out by us and will be the subject of a future publication.

By using  $\text{CH}_3\text{CN}$  instead of  $\text{SO}_2$  as solvent for the reactions of  $\text{NbF}_5$  and  $\text{TaF}_5$  with excess  $(\text{CH}_3)_3\text{SiN}_3$ , yellow solutions of  $\text{CH}_3\text{CN}\cdot\text{Nb}(\text{N}_3)_5$  and  $\text{CH}_3\text{CN}\cdot\text{Ta}(\text{N}_3)_5$ , respectively, were obtained [Eq. (2) (M = Nb, Ta)].



Removal of the volatile compounds ( $\text{CH}_3\text{CN}$ ,  $(\text{CH}_3)_3\text{SiF}$  and excess  $(\text{CH}_3)_3\text{SiN}_3$ ) at  $-20^\circ\text{C}$  results in the isolation of the acetonitrile-adducts of the pentaazides. Although still dangerous and explosive, both acetonitrile-adducts are less shock-sensitive than the corresponding donor-free pentaazides.

Both acetonitrile-adducts were isolated as yellow solids and were characterized by vibrational spectroscopy, their conversion with  $\text{N}_3^-$  into the hexaazido-metalates and, in the case of  $\text{CH}_3\text{CN}\cdot\text{Nb}(\text{N}_3)_5$ , by its crystal structure.<sup>[33]</sup> The observed Raman spectra of  $\text{CH}_3\text{CN}\cdot\text{Nb}(\text{N}_3)_5$  and  $\text{CH}_3\text{CN}\cdot\text{Ta}(\text{N}_3)_5$  are shown in Figures 1 and S3, respectively, and their frequencies and intensities are given in the Experimental Section. A comparison with the calculated spectra is given in Tables S3 and S4 of the Supplementary Material, and the given assignments are in accord with those previously reported<sup>[34,35]</sup> for the related  $\text{CH}_3\text{CN}\cdot\text{SbF}_5$  adduct.

$\text{CH}_3\text{CN}\cdot\text{Nb}(\text{N}_3)_5$  crystallizes in the monoclinic space group  $P2(1)/c$ . The X-ray structure analysis<sup>[33]</sup> (Figure 2) reveals the presence of isolated  $\text{CH}_3\text{CN}\cdot\text{Nb}(\text{N}_3)_5$  units. The closest  $\text{Nb}\cdots\text{N}$  and  $\text{N}\cdots\text{N}$  contacts between neighboring molecules are 3.98 Å and 3.04 Å, respectively.

The molecule consists of a pseudo-octahedral  $\text{NbN}_6$  skeleton with  $\text{CH}_3\text{CN}$  and one azido group in the axial positions. The equatorial positions are occupied by the remaining 4 azido groups which, interestingly, are all bent away from the axial azido ligand. The axial  $\text{Nb}-\text{N}_3$  distance is about 0.09 Å shorter than the four equatorial ones. The most interesting feature, however, is the fact that the axial azido group exhibits a large  $\text{Nb}-\text{N}-\text{NN}$  bond angle of  $168.8(3)^\circ$ , compared to an average angle of  $137.8^\circ$  for the four equatorial ligands, and suggests the presence of a tridative azido ligand. The small deviation of the observed axial  $\text{Nb}-\text{N}-\text{N}$  angle from the ideal  $180^\circ$  is attributed to solid state effects, because our theoretical calculations for the free gaseous molecule at the B3LYP and MP2 levels of theory with an SBKJ+(d) basis set resulted in

Nb-N-N angles of 179.6° and 178.3°, respectively. For free CH<sub>3</sub>CN·Ta(N<sub>3</sub>)<sub>5</sub>, analogous calculations gave values of 179.6 and 180.0°. The significant shortening of the axial Nb-N<sub>3</sub> distance might be attributed to a *trans*-effect caused by the opposite long Nb-NCCH<sub>3</sub> bond.

The average Nb-N<sub>azide</sub> distance of 1.997 Å in CH<sub>3</sub>CN·Nb(N<sub>3</sub>)<sub>5</sub> is significantly shorter than those of 2.081 Å and 2.105 Å found for the terminal azides of two isomers of [Cp\*NbCl(N<sub>3</sub>)(μ-N<sub>3</sub>)]<sub>2</sub>(μ-O)<sup>[16]</sup> and 2.27 Å found for the cluster [Nb<sub>6</sub>Br<sub>12</sub>(N<sub>3</sub>)<sub>6</sub>]<sup>4-</sup>,<sup>[18]</sup> but slightly longer than that of 1.92 Å found in [NbCl<sub>5</sub>(N<sub>3</sub>)]<sup>-</sup><sup>[19]</sup> and is attributed to varying degrees of ionicity of the azide ligands in these compounds.

The reactions of the pentaazides with ionic azides, such as [P(C<sub>6</sub>H<sub>5</sub>)<sub>4</sub>]<sup>+</sup>N<sub>3</sub><sup>-</sup>, in CH<sub>3</sub>CN solution produce the corresponding [Nb(N<sub>3</sub>)<sub>6</sub>]<sup>-</sup> and [Ta(N<sub>3</sub>)<sub>6</sub>]<sup>-</sup> salts, respectively, [Eq. (3) (M = Nb, Ta)].



The hexaazido niobates and tantalates were isolated as yellow-orange solids and are stable at room temperature. The compounds were characterized by the observed material balances, vibrational spectroscopy, and in the case of [P(C<sub>6</sub>H<sub>5</sub>)<sub>4</sub>][Nb(N<sub>3</sub>)<sub>6</sub>] by its crystal structure.<sup>[36]</sup> The observed vibrational spectra of [P(C<sub>6</sub>H<sub>5</sub>)<sub>4</sub>][Nb(N<sub>3</sub>)<sub>6</sub>] and [P(C<sub>6</sub>H<sub>5</sub>)<sub>4</sub>][Ta(N<sub>3</sub>)<sub>6</sub>] are shown in Figures S4 and S5, respectively, and their frequencies and intensities are given in Table 2 and the Experimental Section, respectively. The free gaseous [Nb(N<sub>3</sub>)<sub>6</sub>]<sup>-</sup> anion is predicted to have perfect *S*<sub>6</sub> (≡ *C*<sub>3*i*</sub>) symmetry, which is quite rare,<sup>[37]</sup> and, therefore, a complete vibrational analysis was carried out (Table 2). [Ta(N<sub>3</sub>)<sub>6</sub>]<sup>-</sup> is slightly distorted from *S*<sub>6</sub> to *C*<sub>1</sub> symmetry, but its structure is almost identical to that of [Nb(N<sub>3</sub>)<sub>6</sub>]<sup>-</sup>, and the splittings of its degenerate modes are extremely small (Table S5 of the Supplementary Material).

Because of the presence of a large counter-ion which serves as an inert spacer and suppresses detonation propagation, these salts are much less shock sensitive than neat  $\text{Nb}(\text{N}_3)_5$  and  $\text{Ta}(\text{N}_3)_5$ , and are thermally surprisingly stable. Single crystals of  $[\text{P}(\text{C}_6\text{H}_5)_4][\text{Nb}(\text{N}_3)_6]$  were obtained by re-crystallization from  $\text{CH}_3\text{CN}$ . The salt crystallizes in the rare orthorhombic space group  $P2(1)2(1)2$ . The X-ray structure analysis<sup>[36]</sup> of  $[\text{P}(\text{C}_6\text{H}_5)_4][\text{Nb}(\text{N}_3)_6]$  (Figure 3) reveals no significant cation-anion and anion-anion interactions. The closest  $\text{Nb}\cdots\text{N}$  and  $\text{N}\cdots\text{N}$  contacts between neighboring anions are 4.20 Å and 3.15 Å, respectively. The structure of the  $[\text{Nb}(\text{N}_3)_6]^-$  anion in the solid is distorted from the perfect  $S_6$  symmetry, predicted by our theoretical calculations for the free gaseous anion, and is similar to those of  $[\text{As}(\text{N}_3)_6]^{-[28]}$ ,  $[\text{Sb}(\text{N}_3)_6]^{-[27]}$ ,  $[\text{Si}(\text{N}_3)_6]^{-[38]}$ ,  $[\text{Ge}(\text{N}_3)_6]^{-[39]}$  and  $[\text{Ti}(\text{N}_3)_6]^{2-,[1]}$  and contrary to that of  $[\text{Te}(\text{N}_3)_6]^{2-,[40]}$  which contains a sterically active free valence electron pair on its central atom. The average Nb-N distance of 2.027 Å in  $[\text{Nb}(\text{N}_3)_6]^-$  is larger than that of 1.997 Å found for  $\text{CH}_3\text{CN}\cdot\text{Nb}(\text{N}_3)_5$ , as expected from the formal negative charge in the former which increases the ionic character of the azide ligands. The relatively large variation in the Nb-N-N bond angles, which range from 131.7 to 156.2 °, is attributed to intramolecular repulsion effects among the ligands.

In summary, this paper reports the synthesis and characterization of the first examples of binary Group 5 azides and provides the first experimental proof for the existence of linear metal-N-N bonds.

### ***Experimental Section***

***Caution!*** Covalent azides are potentially hazardous and can decompose explosively under various conditions! The polyazides of this work are extremely shock-sensitive and can explode violently upon the slightest provocation. They should be handled only on a scale of less

than 1 mmol. Because of the high energy content and high detonation velocities of these azides, their explosions are particularly violent and can cause, even on a one mmol scale, significant damage. The use of appropriate safety precautions (safety shields, face shields, leather gloves, protective clothing, such as heavy leather welding suits and ear plugs) is mandatory. Teflon containers should be used, whenever possible, to avoid hazardous shrapnel formation. The manipulation of these materials is facilitated by handling them, whenever possible, in solution to avoid detonation propagation, the use of large inert counter-ions as spacers, and anion formation which increases the partial negative charges on the terminal  $N_\gamma$  atoms and thereby reduces the  $N_\beta$ - $N_\gamma$  triple bond character and strengthens the weak  $N_\alpha$ - $N_\beta$  single bond. **Ignoring safety precautions can lead to serious injuries!**

*Materials and Apparatus:* All reactions were carried out in Teflon-FEP ampules that were closed by stainless steel valves. Volatile materials were handled in a Pyrex glass or stainless steel/Teflon-FEP vacuum line.<sup>[41]</sup> All reaction vessels were passivated with  $\text{ClF}_3$  prior to use. Nonvolatile materials were handled in the dry argon atmosphere of a glove box.

Raman spectra were recorded directly in the Teflon reactors in the range  $3600\text{--}80\text{ cm}^{-1}$  on a Bruker Equinox 55 FT-RA spectrophotometer, using a Nd-YAG laser at 1064 nm with power levels less than 50 mW(!). Infrared spectra were recorded in the range  $4000\text{--}400\text{ cm}^{-1}$  on a Midac, M Series, FT-IR spectrometer using KBr pellets. The pellets were prepared inside the glove box using an Econo mini-press (Barnes Engineering Co.) and transferred in a closed container to the spectrometer before placing them quickly into the sample compartment which was purged with dry nitrogen to minimize exposure to atmospheric moisture and potential hydrolysis of the sample.



The starting materials NbF<sub>5</sub>, TaF<sub>5</sub> (both Ozark Mahoning) and [P(C<sub>6</sub>H<sub>5</sub>)<sub>4</sub>]I (Aldrich) were used without further purification. (CH<sub>3</sub>)<sub>3</sub>SiN<sub>3</sub> (Aldrich) was purified by fractional condensation prior to use. Solvents were dried by standard methods and freshly distilled prior to use. [P(C<sub>6</sub>H<sub>5</sub>)<sub>4</sub>]N<sub>3</sub> and [P(C<sub>6</sub>H<sub>5</sub>)<sub>4</sub>]F were prepared from [P(C<sub>6</sub>H<sub>5</sub>)<sub>4</sub>]I and stoichiometric amounts of AgN<sub>3</sub> and AgF, respectively, in aqueous solution, filtering off the precipitated AgI .

*Preparation of M(N<sub>3</sub>)<sub>5</sub> (M = Nb, Ta):* A sample of NbF<sub>5</sub> (0.55 mmol) or TaF<sub>5</sub> (0.59 mmol) was loaded into a Teflon-FEP ampule, followed by the addition of 1 g of SO<sub>2</sub> and (CH<sub>3</sub>)<sub>3</sub>SiN<sub>3</sub> (5.5 mmol) *in vacuo* at -196 °C. The mixture was warmed to -30 °C. After 2 hours, the temperature was raised to -20 °C and all volatile material was pumped off, leaving behind solid M(N<sub>3</sub>)<sub>5</sub>.

Nb(N<sub>3</sub>)<sub>5</sub>: 0.175 g, expected for 0.55 mmol: 0.166 g; Raman (-80 °C):  $\tilde{\nu}$ =2155 [10.0], 2106 [5.5], ( $\nu_{as}$  N<sub>3</sub>), 1385 [1.6], ( $\nu_s$  N<sub>3</sub>), 628 [0.7], 590 sh, ( $\delta$  N<sub>3</sub>), 427 sh, ( $\nu_{as}$  NbN<sub>3</sub> *eq*), 413 [3.2], ( $\nu_s$  NbN<sub>3</sub> *eq*), 360 sh, ( $\nu_s$  NbN<sub>2</sub> *ax*), 288 [0.7], ( $\delta_{sciss}$  NbN<sub>3</sub> *eq*), 234 [0.7], ( $\rho$  NbN<sub>2</sub> *ax*); infrared (KBr): 2124 vs, 2088 vs, ( $\nu_{as}$  N<sub>3</sub>), 1374 m, 1347 s, ( $\nu_s$  N<sub>3</sub>), 591 mw, 569 w, ( $\delta$  N<sub>3</sub>), 450 sh, ( $\nu_{as}$  NbN<sub>3</sub> *eq*), 440 mw, ( $\nu_{as}$  NbN<sub>2</sub> *ax*), 422 w, ( $\nu_s$  NbN<sub>3</sub> *eq*).

Ta(N<sub>3</sub>)<sub>5</sub>: 0.247 g, expected for 0.59 mmol = 0.231 g; Raman (-80 °C):  $\tilde{\nu}$ =2182 [10.0], 2129 [3.3], ( $\nu_{as}$  N<sub>3</sub>), 623 [1.1], 590 sh, ( $\delta$  N<sub>3</sub>), 450 sh, ( $\nu_{as}$  TaN<sub>3</sub> *eq*), 426 [2.5], ( $\nu_s$  TaN<sub>3</sub> *eq*), 390 sh, ( $\nu_s$  TaN<sub>2</sub> *ax*), 256 [1.7] ( $\delta_{sciss}$  TaN<sub>3</sub> *eq*), 221 [2.0], ( $\rho$  TaN<sub>2</sub> *ax*); infrared (KBr): 2141 vs, 2103vs, ( $\nu_{as}$  N<sub>3</sub>), 1403 ms, 1364 m, ( $\nu_s$  N<sub>3</sub>), 613 mw, 578 w, ( $\delta$  N<sub>3</sub>), 410 mw, ( $\nu_{as}$  TaN<sub>2</sub> *ax*).

In addition to these bands, the following weak infrared bands were observed which are attributed to overtones or combination bands: Nb(N<sub>3</sub>)<sub>5</sub>: 1667 w, 1263 w, 1195 sh, 1176 w, 1037 vvw, 696 w, 660 w; Ta(N<sub>3</sub>)<sub>5</sub>: 1669 w, 1508 vw, 1274 sh, 1252 w, 1203 w, 1180 sh, 1036 vw, 850 w, 712 w, 683 w.

*Preparation of  $\text{CH}_3\text{CN}\cdot\text{M}(\text{N}_3)_5$  ( $M = \text{Nb}, \text{Ta}$ ):* A sample of  $\text{NbF}_5$  (0.39 mmol) or  $\text{TaF}_5$  (0.37 mmol) was loaded into a Teflon-FEP ampule, followed by the addition of 2 mL  $\text{CH}_3\text{CN}$  and  $(\text{CH}_3)_3\text{SiN}_3$  (3.7 mmol) *in vacuo* at  $-196^\circ\text{C}$ . The mixture was warmed to  $-20^\circ\text{C}$ . After 2 hours, all volatile material was pumped off at this temperature, leaving behind solid  $\text{CH}_3\text{CN}\cdot\text{M}(\text{N}_3)_5$ .

$\text{CH}_3\text{CN}\cdot\text{Nb}(\text{N}_3)_5$ : 0.129 g, expected for 0.39 mmol: 0.136 g. Raman ( $-80^\circ\text{C}$ ):  $\tilde{\nu}=2928$  [1.8], ( $\nu_s \text{CH}_3$ ), 2315 [1.2], 2289 [1.1], ( $\nu \text{CN}$ ), 2140 [10.0], 2121 [1.5], 2097 [1.9], 2090 [1.6], 2074 [2.2], 2058 [1.4], ( $\nu_{\text{as}} \text{N}_3$ ), 1415 [1.3], 1363 [1.2], 1351 [1.1], 1331 [1.1], ( $\delta \text{CH}_3$ ) and ( $\nu_s \text{N}_3$ ), 947 [1.0], ( $\nu \text{CC}$ ), 620 [1.2], 610 [1.0], 599 [1.2], 580 [1.1], 566 [1.0], 557 [1.1], ( $\delta \text{N}_3$ ), 441 [3.1], 435 [2.8], 423 [1.7], 419 [1.7], 411 [2.0], ( $\nu \text{NbN}_x$ ), 281 [1.1], 266 [1.3], 256 [1.3], 248 [1.4], 226 [1.6], ( $\delta \text{NbN}_x$ ), 189 [1.3], 180 [1.3], 139 [1.6], 96 [2.9], (torsional modes).

$\text{CH}_3\text{CN}\cdot\text{Ta}(\text{N}_3)_5$ : 0.175 g, expected for 0.37 mmol: 0.161 g. Raman ( $-80^\circ\text{C}$ ):  $\tilde{\nu}=2933$  [1.7], ( $\nu_s \text{CH}_3$ ), 2319 [0.5], 2291 [0.5], ( $\nu \text{CN}$ ), 2172 [10.0], 2162 [1.2], 2123 [1.2], 2103 [1.1], ( $\nu_{\text{as}} \text{N}_3$ ), 1389 [0.4], 1361 [0.4], ( $\delta \text{CH}_3$ ) and ( $\nu_s \text{N}_3$ ), 948 [1.0], ( $\nu \text{CC}$ ), 592 [0.3], ( $\delta \text{N}_3$ ), 438 [2.1], 417 [0.6], ( $\nu \text{NbN}_x$ ), 250 [0.7], 266 [1.3], 226 [0.6], ( $\delta \text{NbN}_x$ ), 192 [0.9], (torsional mode).

*Preparation of  $[\text{M}(\text{N}_3)_6]^-$  salts ( $M = \text{Nb}, \text{Ta}$ ):* Neat  $\text{PPh}_4\text{N}_3$  (0.25 mmol) was added to a frozen solution of  $\text{M}(\text{N}_3)_5$  (0.25 mmol) in  $\text{CH}_3\text{CN}$  (15 mmol) at  $-78^\circ\text{C}$ . The reaction mixture was warmed to  $-25^\circ\text{C}$  and occasionally agitated. After 2 hours, all volatiles were removed at ambient temperature in a dynamic vacuum, leaving behind the solid  $[\text{M}(\text{N}_3)_6]^-$  salts.

$[\text{P}(\text{C}_6\text{H}_5)_4][\text{Nb}(\text{N}_3)_6]^-$ : orange solid, 0.160 g, expected for 0.25 mmol: 0.171 g. The IR and Raman spectra of  $[\text{Nb}(\text{N}_3)_6]^-$  are given in Table1.

$[\text{P}(\text{C}_6\text{H}_5)_4][\text{Ta}(\text{N}_3)_6]^-$ : pale yellow solid, 0.207 g, expected for 0.25 mmol: 0.193 g. Raman bands due to  $[\text{Ta}(\text{N}_3)_6]^-$  ( $-80^\circ\text{C}$ ):  $\tilde{\nu}=2159$  [10.0], 2111 [1.0], 2103 [1.0], 2091 [0.8], 2081 [0.7],

( $\nu_{\text{as}} \text{N}_3$ ), 1355 [0.8], ( $\nu_{\text{s}} \text{N}_3$ ), 609 [0.6], 582 [0.4], ( $\delta \text{N}_3$ ), 437 [2.8], 372 [0.7], 364 [0.8], 353 [0.8], ( $\nu \text{TaN}_6$ ), 225 [1.8], 215 [1.8], ( $\delta \text{TaN}_6$ ), 168 [2.6], 160 [2.6], (torsions); infrared bands due to  $[\text{Ta}(\text{N}_3)_6]^-$  (KBr): 2124 vs, 2113 vs, 2096 vs, 2087 vs, ( $\nu_{\text{as}} \text{N}_3$ ), 1383 m, 1372 m, 1360 ms, 1348 s, ( $\nu_{\text{s}} \text{N}_3$ ), 648 vw, 615 m, 600 mw, 585 mw, 576 w, ( $\delta \text{N}_3$ ), 433 w, 418 mw, 414 mw, ( $\nu \text{TaN}_6$ ).

*Theoretical Methods:* The molecular structures, harmonic vibrational frequencies, and infrared and Raman vibrational intensities were calculated using second order perturbation theory (MP2, also known as MBPT(2)<sup>[24]</sup>) and also at the DFT level using the B3LYP hybrid functional,<sup>[23a]</sup> which included the VWN5 correlation functional.<sup>[23b]</sup> The Stevens, Basch, Krauss, and Jasien (SBKJ) effective core potentials and the corresponding valence-only basis sets were used.<sup>[25a]</sup> The SBKJ valence basis set for nitrogen was augmented with a d polarization function<sup>[25b]</sup> and a diffuse s+p shell,<sup>[25c]</sup> denoted as SBKJ+(d). Hessians (energy second derivatives) were calculated for the final equilibrium structures to verify them as local minima; i.e., having a positive definite Hessian. All calculations were performed using the electronic structure code GAMESS.<sup>[42]</sup>

Received: , 2005

**Keywords:** Crystal structure, hexaazidoniobate(V), hexaazidotantalate(V), niobium pentaazide, niobium pentaazide - acetonitrile adduct, tantalum pentaazide, tantalum pentaazide – acetonitrile adduct, vibrational spectra, binary Group 5 azides, theoretical calculations, linear metal-nitrogen-nitrogen bonds

## References

- [1] R. Haiges, J. A. Boatz, S. Schneider, T. Schroer, K. O. Christe, *Angew. Chem. Int. Ed.* **2004**, *43*, 3148.
- [2] R. Haiges, J. A. Boatz, R. Bau, S. Schneider, T. Schroer, M. Yousufuddin, K. O. Christe, *Angew. Chem. Int. Ed.* **2005**, *44*, 1860.
- [3] A. Kornath, *Angew. Chem. Int. Ed.* **2001**, *40*, 3135 and references cited therein.
- [4] K. Dehnicke, J. Strähle, *Z. Anorg. Allg. Chem.* **1965**, *338*, 287.
- [5] K. Dehnicke, *J. Inorg. Nucl. Chem.* **1965**, *27*, 809.
- [6] J. Strähle, *Z. Anorg. Allg. Chem.* **1974**, *405*, 139.
- [7] R. Choukroun, D. Gervais, *J. Chem. Soc., Dalton Trans.* **1980**, 1800.
- [8] U. Müller, R. Dübgen, K. Dehnicke, *Z. Anorg. Allg. Chem.* **1981**, *473*, 115.
- [9] a) W. Beck, E. Schuierer, P. Poellmann, W. P. Fehlhammer, *Z. Naturforsch. B*, **1966**, *21*, 811; b) W. Beck, W. P. Fehlhammer, P. Poellmann, E. Schuierer, K. Feldl, *Chem. Ber.* **1967**, *100*, 2335.
- [10] D. B. Sable, W. H. Armstrong, *Inorg. Chem.* **1992**, *31*, 161.
- [11] J. H. Espenson, J. R. Pladziewicz, *Inorg. Chem.* **1970**, *9*, 1380.
- [12] M. Kasper, R. Bereman, *Inorg. Nucl. Chem. Let.* **1974**, *10*, 443.
- [13] M. Herberhold, A.-M. Dietel, W. Milius, *Z. Anorg. Allg. Chem.* **1999**, *625*, 1885.
- [14] J. H. Osborne, A. L. Rheingold, W. C. Trogler, *J. Am. Chem. Soc.* **1985**, *107*, 7945.
- [15] M. Herberhold, A. Goller, W. Milius, *Z. Anorg. Allg. Chem.* **2003**, *629*, 1162.
- [16] M. Herberhold, A. Goller, W. Milius, *Z. Anorg. Allg. Chem.* **2003**, *629*, 1557.
- [17] M. Herberhold, A. Goller, W. Milius, *Z. Anorg. Allg. Chem.* **2001**, *627*, 891.
- [18] J. H. Meyer, *Z. Anorg. Allg. Chem.* **1995**, *621*, 921.

- [19] O. Reckeweg, H.-J. Meyer, A. Simon, *Z. Anorg. Allg. Chem.* **2002**, 628, 920.
- [20] H.-J. Meyer, *Z. Anorg. Allg. Chem.* **1995**, 621, 921.
- [21] R. Dübgen, U. Müller, F. Weller, K. Dehnicke, *Z. Anorg. Allg. Chem.* **1980**, 471, 89.
- [22] A. M. Golub, H. Köhler, V. V. Stopenko, *Chemistry of Pseudohalides*, Elsevier, Amsterdam, **1986**.
- [23] a) A. D. Becke, *J. Chem. Phys.* **1993**, 98, 5648; P. J. Stephens, F. J. Devlin, C. F. Chablowski, M. J. Frisch, *J. Phys. Chem.* **1994**, 98, 11623; R. H. Hertwig, W. Koch, *Chem. Phys. Lett.* **1997**, 268, 345.  
b) S. H. Vosko, L. Wilk, M. Nusair, *Can. J. Phys.* **1980**, 58, 1200.
- [24] C. Moller, M. S. Plesset, *Phys. Rev.* **1934**, 46, 618; J. A. Pople, J. S. Binkley, R. Seeger, *Int. J. Quantum Chem. S10*, **1976**, 1; M. J. Frisch, M. Head-Gordon, J. A. Pople, *Chem. Phys. Lett.* **1990**, 166, 275; R. J. Bartlett, D. M. Silver, *Int. J. Quantum Chem. Symp.* **1975**, 9, 1927.
- [25] a) W. J. Stevens, H. Basch, M. Krauss, *J. Chem. Phys.* **1984**, 81, 6026; W. J. Stevens, M. Krauss, H. Basch, P. G. Jasien, *Can. J. Chem.* **1992**, 70, 612.  
b) P. C. Hariharan, J. A. Pople, *Theoret. Chim. Acta* **1973**, 28, 213.  
c) T. Clark, J. Chandrasekhar, G. W. Spitznagel, P. von R. Schleyer, *J. Comput. Chem.* **1983**, 4, 294.
- [26] J. Drummond, J. S. Wood, *J. Chem. Soc., Chem. Commun.* **1969**, 1373.
- [27] R. Haiges, J. A. Boatz, A. Vij, V. Vij, M. Gerken, S. Schneider, T. Schroer, M. Yousufuddin, K. O. Christe, *Angew. Chem. Int. Ed.* **2004**, 43, 6676.

- [28] a) K. Karaghiosoff, T. M. Klapötke, B. Krumm, H. Nöth, T. Schütt, M. Suter, *Inorg. Chem.* **2002**, *41*, 170; b) T. M. Klapötke, H. Nöth, T. Schütt, M. Warchhold, *Angew. Chem. Int. Ed.* **2000**, *39*, 2108.
- [29] (a) R. J. Gillespie, I. Hargittai, *The VSEPR Model of Molecular Geometry*, Allyn and Bacon, A Division of Simon & Schuster, Inc.: Needham Heights, MA, **1991**; (b) R. J. Gillespie, P. L. A. Popelier, *Chemical Bonding and Molecular Geometry: from Lewis to Electron Densities*, Oxford University Press, **2001**.
- [30] L. Gagliardi, P. Pyykkoe, *Inorg. Chem.* **2003**, *42*, 3074.
- [31] M. Teichert, J. A. Boatz, private communication.
- [32] P. H. Bird, M. R. Churchill, *Chem. Commun.* **1967**, 403.
- [33] Crystal data for  $C_2H_3N_{16}Nb$ :  $M_r = 344.11$ , monoclinic, space group  $P2(1)/c$ ,  $a = 7.9805(12)$ ,  $b = 10.4913(16)$ ,  $c = 14.695(2)$  Å,  $\alpha = 90$ ,  $\beta = 96.353(2)$ ,  $\gamma = 90^\circ$ ,  $V = 1222.8(3)$  Å<sup>3</sup>,  $F(000) = 672$ ,  $\rho_{calcd.}$  ( $Z = 4$ ) =  $1.869 \text{ g}\cdot\text{cm}^{-3}$ ,  $\mu = 1.004 \text{ mm}^{-1}$ , approximate crystal dimensions  $0.25 \times 0.08 \times 0.02 \text{ mm}^3$ ,  $\theta$  range =  $2.39$  to  $27.48^\circ$ ,  $Mo_{K\alpha}$  ( $\lambda = 0.71073$  Å),  $T = 163(2)$  K, 3392 measured data (Bruker 3-circle, SMART APEX CCD with  $\chi$ -axis fixed at  $54.74^\circ$ , using the SMART V 5.625 program, Bruker AXS: Madison, WI, 2001), of which 839 ( $R_{int} = 0.0204$ ) unique. Lorentz and polarization correction (SAINT V 6.22 program, Bruker AXS: Madison, WI, 2001), absorption correction (SADABS program, Bruker AXS: Madison, WI, 2001). Structure solution by direct methods (SHELXTL 5.10, Bruker AXS: Madison, WI, 2000), full-matrix least-squares refinement on  $F^2$ , data to parameters ratio: 15.9 : 1, final  $R$  indices [ $I > 2\sigma(I)$ ]:  $R1 = 0.0341$ ,  $wR2 = 0.0692$ ,  $R$  indices (all data):  $R1 = 0.0546$ ,  $wR2 = 0.0746$ , GOF on  $F^2 = 1.003$ . Further crystallographic details can be obtained from the Cambridge Crystallographic Data

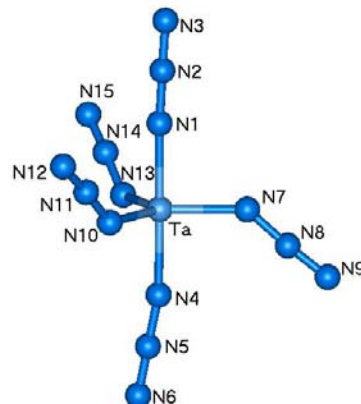
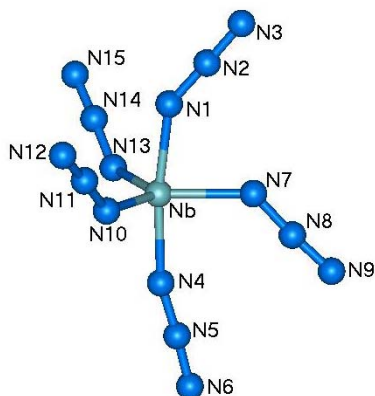
Centre (CCDC, 12 Union Road, Cambridge CB21EZ, UK (Fax: (+44) 1223-336-033; e-mail: [deposit@ccdc.cam.ac.uk](mailto:deposit@ccdc.cam.ac.uk)) on quoting the deposition no. CCDC 246594.

- [34] B. v. Ahsen, B. Bley, S. Proemmel, R. Wartchow, H. Willner, F. Aubke, *Z. Anorg. Allg. Chem.* **1998**, 624, 1225.
- [35] D. M. Byler, D. F. Shriver, *Inorg. Chem.* **1973**, 12, 1412 and **1974**, 13, 2697.
- [36] Crystal data for  $C_{24}H_{20}N_{18}NbP$ :  $M_r = 684.46$ , orthorhombic, space group  $P2(1)2(1)2$ ,  $a = 18.480(3)$ ,  $b = 23.153(4)$ ,  $c = 6.7831(13)$  Å,  $\alpha = 90$ ,  $\beta = 90$ ,  $\gamma = 90^\circ$ ,  $V = 2902.3(9)$  Å<sup>3</sup>,  $F(000) = 1384$ ,  $\rho_{calcd.}$  ( $Z = 4$ ) =  $1.566 \text{ g}\cdot\text{cm}^{-3}$ ,  $\mu = 0.521 \text{ mm}^{-1}$ , approximate crystal dimensions  $0.33 \times 0.05 \times 0.04 \text{ mm}^3$ ,  $\theta$  range =  $1.41$  to  $27.51^\circ$ ,  $MoK\alpha$  ( $\lambda = 0.71073$  Å),  $T = 133(2)$  K, 17936 measured data (Bruker 3-circle, SMART APEX CCD with  $\chi$ -axis fixed at  $54.74^\circ$ , using the SMART V 5.625 program, Bruker AXS: Madison, WI, 2001), of which 6575 ( $R_{int} = 0.0597$ ) unique. Lorentz and polarization correction (SAINT V 6.22 program, Bruker AXS: Madison, WI, 2001), absorption correction (SADABS program, Bruker AXS: Madison, WI, 2001). Structure solution by direct methods (SHELXTL 5.10, Bruker AXS: Madison, WI, 2000), full-matrix least-squares refinement on  $F^2$ , data to parameters ratio: 16.5 : 1, final  $R$  indices [ $I > 2\sigma(I)$ ]:  $R1 = 0.0518$ ,  $wR2 = 0.0936$ ,  $R$  indices (all data):  $R1 = 0.0858$ ,  $wR2 = 0.1049$ , GOF on  $F^2 = 1.028$ . Further crystallographic details can be obtained from the Cambridge Crystallographic Data Centre (CCDC, 12 Union Road, Cambridge CB21EZ, UK (Fax: (+44) 1223-336-033; e-mail: [deposit@ccdc.cam.ac.uk](mailto:deposit@ccdc.cam.ac.uk)) on quoting the deposition no. CCDC 251934.
- [37] J. Weidlein, U. Mueller, K. Dehnicke, *Schwingungsspektroskopie*, Georg Thieme Verlag, Stuttgart-New York, **1982**, pg. 102.
- [38] A. C. Filippou, P. Portius, G. Schnakenburg, *J. Am. Chem. Soc.* **2002**, 124, 12396.

- [39] A. C. Filippou, P. Portius, D. U. Neumann, K.-D. Wehrstedt, *Angew. Chem. Int. Ed.* **2000**, *39*, 4333.
- [40] T. M. Klapoetke, H. Noeth, T., T. Schuett, M. Warchhold, *Angew. Chem. Int. Ed.* **2000**, *39*, 2108.
- [41] K. O. Christe, W. W. Wilson, C. J. Schack, R. D. Wilson, *Inorg. Synth.* **1986**, *24*, 39.
- [42] M. W. Schmidt, K. K. Baldridge, J. A. Boatz, S. T. Elbert, M. S. Gordon, J. H. Jensen, S. Koseki, N. Matsunaga, K. A. Nguyen, S. J. Su, T. L. Windus, M. Dupuis, J. A. Montgomery, *J. Comput. Chem.* **1993**, *14*, 1347.



**Table 1.** Structures of Nb(N<sub>3</sub>)<sub>5</sub> and Ta(N<sub>3</sub>)<sub>5</sub> calculated at the B3LYP/SBKJ+(d) level of theory (MP2/SBKJ+(d) values in parentheses).



$R(\text{Nb}-\text{N}_1)$	$= 2.025(2.013)$
$R(\text{Nb}-\text{N}_4)$	$= 2.001(2.002)$
$R(\text{Nb}-\text{N}_7)$	$= 2.048(2.060)$
$R(\text{Nb}-\text{N}_{10})$	$= 2.008(2.014)$
$R(\text{Nb}-\text{N}_{13})$	$= 2.008(2.014)$
$R(\text{N}_1-\text{N}_2)$	$= 1.234(1.241)$
$R(\text{N}_4-\text{N}_5)$	$= 1.230(1.241)$
$R(\text{N}_7-\text{N}_8)$	$= 1.243(1.249)$
$R(\text{N}_{10}-\text{N}_{11})$	$= 1.240(1.245)$
$R(\text{N}_{13}-\text{N}_{14})$	$= 1.240(1.245)$
$R(\text{N}_2-\text{N}_3)$	$= 1.162(1.208)$
$R(\text{N}_5-\text{N}_6)$	$= 1.163(1.210)$
$R(\text{N}_8-\text{N}_9)$	$= 1.162(1.210)$
$R(\text{N}_{11}-\text{N}_{12})$	$= 1.160(1.208)$
$R(\text{N}_{14}-\text{N}_{15})$	$= 1.160(1.208)$
$\alpha(\text{N}_1-\text{Nb}-\text{N}_4)$	$= 171.9(169.0)$
$\alpha(\text{N}_1-\text{Nb}-\text{N}_7)$	$= 82.8(81.4)$
$\alpha(\text{N}_1-\text{Nb}-\text{N}_{10})$	$= 91.0(92.1)$
$\alpha(\text{N}_1-\text{Nb}-\text{N}_{13})$	$= 91.0(92.1)$
$\alpha(\text{N}_4-\text{Nb}-\text{N}_7)$	$= 89.1(87.6)$
$\alpha(\text{N}_4-\text{Nb}-\text{N}_{10})$	$= 93.2(93.6)$
$\alpha(\text{N}_4-\text{Nb}-\text{N}_{13})$	$= 93.2(93.6)$
$\alpha(\text{N}_7-\text{Nb}-\text{N}_{10})$	$= 121.3(121.3)$
$\alpha(\text{N}_7-\text{Nb}-\text{N}_{13})$	$= 121.3(121.3)$
$\alpha(\text{N}_{10}-\text{Nb}-\text{N}_{13})$	$= 117.2(117.1)$
$\alpha(\text{Nb}-\text{N}_1-\text{N}_2)$	$= 145.3(147.2)$
$\alpha(\text{Nb}-\text{N}_4-\text{N}_5)$	$= 165.0(157.3)$
$\alpha(\text{Nb}-\text{N}_7-\text{N}_8)$	$= 131.8(130.8)$
$\alpha(\text{Nb}-\text{N}_{10}-\text{N}_{11})$	$= 137.2(138.8)$
$\alpha(\text{Nb}-\text{N}_{13}-\text{N}_{14})$	$= 137.2(138.8)$

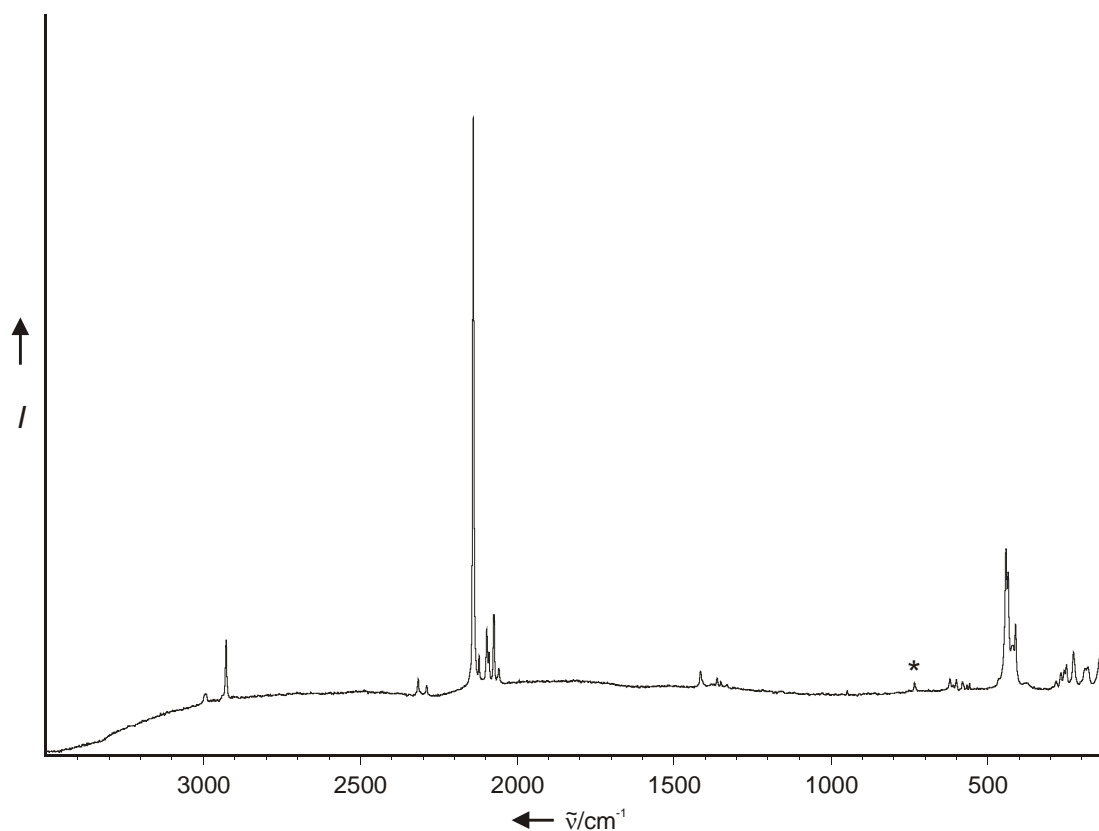
$R(\text{Ta}-\text{N}_1)$	$= 1.997(1.996)$
$R(\text{Ta}-\text{N}_4)$	$= 1.991(1.993)$
$R(\text{Ta}-\text{N}_7)$	$= 2.003(1.997)$
$R(\text{Ta}-\text{N}_{10})$	$= 2.008(2.009)$
$R(\text{Ta}-\text{N}_{13})$	$= 2.008(2.009)$
$R(\text{N}_1-\text{N}_2)$	$= 1.226(1.235)$
$R(\text{N}_4-\text{N}_5)$	$= 1.225(1.234)$
$R(\text{N}_7-\text{N}_8)$	$= 1.240(1.242)$
$R(\text{N}_{10}-\text{N}_{11})$	$= 1.240(1.244)$
$R(\text{N}_{13}-\text{N}_{14})$	$= 1.240(1.244)$
$R(\text{N}_2-\text{N}_3)$	$= 1.163(1.209)$
$R(\text{N}_5-\text{N}_6)$	$= 1.163(1.209)$
$R(\text{N}_8-\text{N}_9)$	$= 1.160(1.206)$
$R(\text{N}_{11}-\text{N}_{12})$	$= 1.160(1.206)$
$R(\text{N}_{14}-\text{N}_{15})$	$= 1.160(1.206)$
$\alpha(\text{N}_1-\text{Ta}-\text{N}_4)$	$= 179.2(177.9)$
$\alpha(\text{N}_1-\text{Ta}-\text{N}_7)$	$= 89.4(90.2)$
$\alpha(\text{N}_1-\text{Ta}-\text{N}_{10})$	$= 90.2(89.8)$
$\alpha(\text{N}_1-\text{Ta}-\text{N}_{13})$	$= 90.2(89.8)$
$\alpha(\text{N}_4-\text{Ta}-\text{N}_7)$	$= 91.4(91.8)$
$\alpha(\text{N}_4-\text{Ta}-\text{N}_{10})$	$= 89.4(89.2)$
$\alpha(\text{N}_4-\text{Ta}-\text{N}_{13})$	$= 89.4(89.2)$
$\alpha(\text{N}_7-\text{Ta}-\text{N}_{10})$	$= 119.6(119.1)$
$\alpha(\text{N}_7-\text{Ta}-\text{N}_{13})$	$= 119.6(119.1)$
$\alpha(\text{N}_{10}-\text{Ta}-\text{N}_{13})$	$= 120.9(121.7)$
$\alpha(\text{Ta}-\text{N}_1-\text{N}_2)$	$= 176.9(178.5)$
$\alpha(\text{Ta}-\text{N}_4-\text{N}_5)$	$= 169.3(173.8)$
$\alpha(\text{Ta}-\text{N}_7-\text{N}_8)$	$= 137.7(143.0)$
$\alpha(\text{Ta}-\text{N}_{10}-\text{N}_{11})$	$= 137.1(138.9)$
$\alpha(\text{Ta}-\text{N}_{13}-\text{N}_{14})$	$= 137.1(138.9)$

Table 2. Comparison of observed and unscaled calculated vibrational frequencies [ $\text{cm}^{-1}$ ] and intensities for  $[\text{Nb}(\text{N}_3)_6]^{-[\text{a}]}$  in point group  $S_6$

description		observed IR	Ra	Calculated (IR) [Raman] B3LYP/SBK+(d) MP2/SBK+(d)	
$A_g$ $\nu_1$	$\nu_{\text{as}}\text{N}_3$		2131 (10.0) 2112 (5.6)	2218 (0) [1428]	2129 (0) [1388]
	$\nu_2$		1342 (2.0)	1432 (0) [49]	1283 (0) [60]
	$\nu_3$		616 (2.8)	588 (0) [8.8]	565 (0) [39]
	$\nu_4$			580 (0) [2.2]	524 (0) [2.3]
	$\nu_5$		433 (5.3) 414 (4.8)	401 (0) [147]	402 (0) [367]
	$\nu_6$		225 (3.5)	249 (0) [13]	242 (0) [51]
	$\nu_7$			74 (0) [14]	72 (0) [31]
	$\nu_8$			34 (0) [37]	32 (0) [39]
$E_g$ $\nu_9$	$\nu_{\text{as}}\text{N}_3$		2080 (2.1) 2060 (2.3)	2164 (0) [1063]	2146 (0) [110]
	$\nu_{10}$			1413 (0) [50]	1279 (0) [154]
	$\nu_{11}$			582 (0) [8.4]	550 (0) [73]
	$\nu_{12}$			580 (0) [0.63]	521 (0) [4.2]
	$\nu_{13}$		339 (2.7)	334 (0) [12]	350 (0) [38]
	$\nu_{14}$		217 (3.5)	238 (0) [34]	234 (0) [31]
	$\nu_{15}$			87 (0) [36]	89 (0) [92]
	$\nu_{16}$			36 (0) [69]	38 (0) [80]
$A_u$ $\nu_{17}$	$\nu_{\text{as}}\text{N}_3$	2121 s 2080 vs		2185 (4084) [0]	2152 (2577) [0]
	$\nu_{18}$	1336 ms		1406 (677) [0]	1271 (338) [0]
	$\nu_{19}$	640 vw		580 (0.91) [0]	549 (100) [0]
	$\nu_{20}$	624 w		574 (49) [0]	505 (8.0) [0]
	$\nu_{21}$	409 mw		400 (536) [0]	418 (629) [0]
	$\nu_{22}$			276 (15) [0]	262 (31) [0]
	$\nu_{23}$			140 (2.8) [0]	114(0.48) [0]
	$\nu_{24}$			27 (0.006) [0]	29 (0.022) [0]
$E_u$ $\nu_{25}$	$\nu_{\text{as}}\text{N}_3$	2069 vs 2060 vs		2170 (4366) [0]	2141 (2681) [0]
	$\nu_{27}$	1361 m 1351 m		1409 (739) [0]	1278 (314) [0]
	$\nu_{28}$	600 w		577 (126) [0]	544 (94) [0]
	$\nu_{29}$	583 vw		570 (38) [0]	502 (8.2) [0]
	$\nu_{30}$	409 mw	382 (2.8)	391 (874) [0]	404 (1045) [0]
	$\nu_{31}$			233 (26) [0]	223 (30) [0]
	$\nu_{32}$		151 (4.3)	154 (13) [0]	128 (31) [0]
	$\nu_{33}$			36 (4.8) [0]	38 (3.1) [0]
$\nu_{34}$	$\tau$			15 (1.6) [0]	6 (1.9) [0]
	$\tau$				

[a] Calculated IR and Raman intensities are given in  $\text{km mol}^{-1}$  and  $\text{\AA}^4 \text{amu}^{-1}$ , respectively; observed spectra are for the solid  $[\text{P}(\text{C}_6\text{H}_5)_4]^+$  salt.

**Figure 1.** Raman spectrum of solid  $\text{CH}_3\text{CN}\cdot\text{Nb}(\text{N}_3)_5$ . The band marked by an asterisk (\*) is due to the Teflon-FEP sample tube.



**Figure 2.** ORTEP drawing of  $\text{CH}_3\text{CN}\cdot\text{Nb}(\text{N}_3)$ . Thermal ellipsoids are shown at the 50% probability level. Selected bond lengths [ $\text{\AA}$ ] and angles [ $^\circ$ ]: Nb-N1 2.031(3), Nb-N4 1.998(3), Nb-N7 2.004(3), Nb-N10 2.017(3), Nb-N13 1.935(3), Nb-N16 2.259(3), N1-N2 1.217(4), N2-N3 1.139(4), N4-N5 1.212(4), N5-N6 1.133(4), N7-N8 1.212(4), N8-N9 1.129(4), N10-N11 1.211(4), N11-N12 1.132(4), N13-N14 1.205(4), N14-N15 1.137(4), N16-C1 1.139(4), C1-C2 1.447(5), N1-Nb-N4 87.55(12), N1-Nb-N7 165.51(11), N1-Nb-N10 82.89(12), N1-Nb-N13 99.16(12), N1-Nb-N16 84.59(10), N4-Nb-N7 93.90(12), N4-Nb-N10 162.91(12), N4-Nb-N13 96.38(12), N4-Nb-N16 81.15(10), N7-Nb-N10 91.93(11), N7-Nb-N13 95.01(12), N7-Nb-N16 81.40(11), N10-Nb-N13 99.11(12), N10-Nb-N16 83.86(10), N13-Nb-N16 175.45(11), Nb-N1-N2 132.7(2), Nb-N4-N5 141.9(2), Nb-N7-N8 144.1(2), Nb-N10-N11 132.3(2), Nb-N13-N14 168.8(3), Nb-N16-C1 170.6(3).

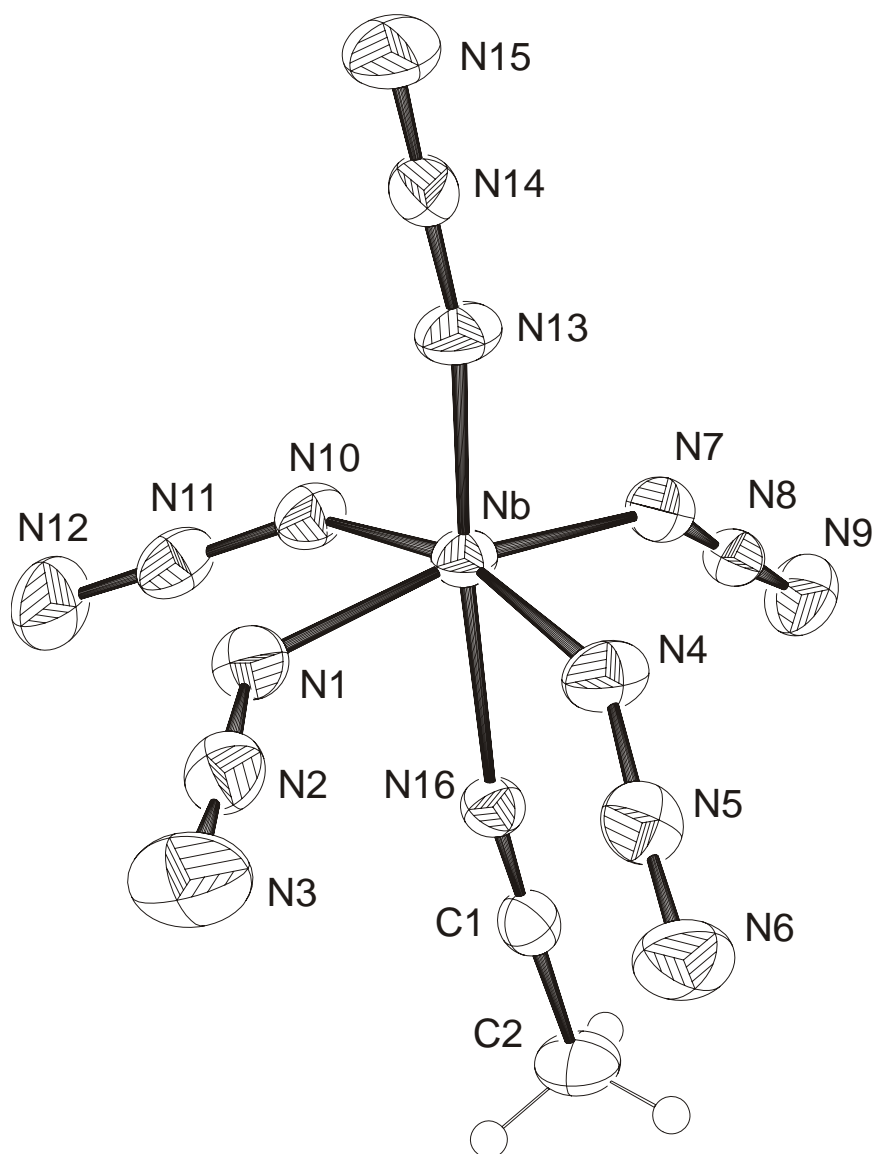
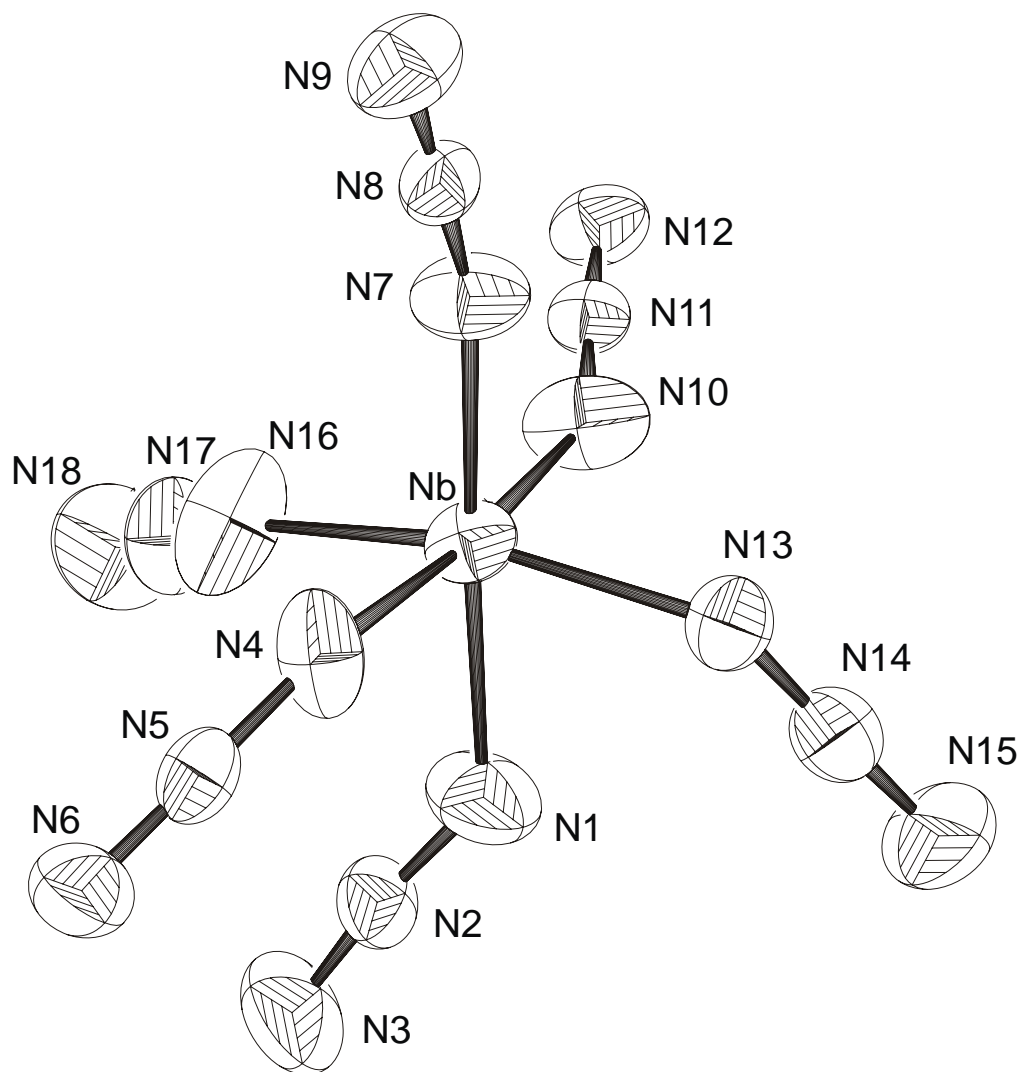


**Figure 3.** ORTEP drawing of the anionic part of the crystal structure of  $[\text{P}(\text{C}_6\text{H}_5)_4][\text{Nb}(\text{N}_3)_6]$ . Thermal ellipsoids are shown at the 50% probability level. Selected bond lengths [ $\text{\AA}$ ] and angles [ $^\circ$ ]: Nb-N1 2.078(5), Nb-N4 2.035(4), Nb-N7 1.989(4), Nb-N10 2.008(4), Nb-N13 2.032(4), Nb-N16 2.026(5), N1-N2 1.164(5), N2-N3 1.126(6), N4-N5 1.198(5), N5-N6 1.128(5), N7-N8 1.192(5), N8-N9 1.133(5), N10-N11 1.196(5), N11-N12 1.118(5), N13-N14 1.203(6), N14-N15 1.137(6), N16-N17 1.173(6), N17-N18 1.137(6), N1-Nb-N4 89.54(19), N1-Nb-N7 173.25(18), N1-Nb-N10 94.23(18), N1-Nb-N13 80.45(18), N1-Nb-N16 85.2(2), N4-Nb-N7 86.30(18), N4-Nb-N10 174.15(18), N4-Nb-N13 95.40(15), N4-Nb-N16 86.78(17), N7-Nb-N10 90.34(17), N7-Nb-N13 94.63(17), N7-Nb-N16 99.86(19), N10-Nb-N13 89.63(18), N10-Nb-N16 89.1(2), N13-Nb-N16 165.46(18), Nb-N1-N2 134.4(4), Nb-N4-N5 141.2(4), Nb-N7-N8 156.2(4), Nb-N10-N11 152.3(4), Nb-N13-N14 131.7(4), Nb-N16-N17 142.3(4).

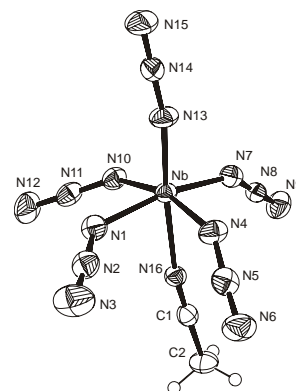


## Synopsis

R. Haiges\*, J. A. Boatz, T. Schroer,  
M. Yousufuddin, K. O. Christe\*

Experimental Evidence for Linear  
Metal-Azide Bonds. The Binary  
Group 5 Azides  $\text{Nb}(\text{N}_3)_5$ ,  $\text{Ta}(\text{N}_3)_5$ ,  
 $[\text{Nb}(\text{N}_3)_6]^-$  and  $[\text{Ta}(\text{N}_3)_6]^-$ , and 1:1  
Adducts of  $\text{Nb}(\text{N}_3)_5$  and  $\text{Ta}(\text{N}_3)_5$   
with  $\text{CH}_3\text{CN}$

**Linear M-N-N bonds:** The first binary  
group 5 azides,  $\text{Nb}(\text{N}_3)_5$ ,  $\text{Ta}(\text{N}_3)_5$ ,  
 $[\text{Nb}(\text{N}_3)_6]^-$  and  $[\text{Ta}(\text{N}_3)_6]^-$ , and 1:1  
adducts of  $\text{Nb}(\text{N}_3)_5$  and  $\text{Ta}(\text{N}_3)_5$  with  
 $\text{CH}_3\text{CN}$ , have been prepared and  
characterized. The crystal structures of  
the  $\text{M}(\text{N}_3)_5 \cdot \text{CH}_3\text{CN}$  adducts provide the  
first experimental evidence for the  
existence of linear metal-N-N bonds.



$\text{CH}_3\text{CN} \cdot \text{Nb}(\text{N}_3)_5$

## Supplementary Material

### Experimental Evidence for Linear Metal-Azide Bonds. The Binary Group 5 Azides $\text{Nb}(\text{N}_3)_5$ , $\text{Ta}(\text{N}_3)_5$ , $[\text{Nb}(\text{N}_3)_6]^-$ and $[\text{Ta}(\text{N}_3)_6]^-$ , and 1:1 Adducts of $\text{Nb}(\text{N}_3)_5$ and $\text{Ta}(\text{N}_3)_5$ with $\text{CH}_3\text{CN}$ \*\*

Ralf Haiges<sup>\*</sup>, Jerry A. Boatz, Thorsten Schroer, Muhammed Yousufuddin, and Karl O. Christe<sup>\*</sup>

Figure S1. IR and Raman spectrum of solid  $\text{Nb}(\text{N}_3)_5$ .

Figure S2. IR and Raman spectra of  $\text{Ta}(\text{N}_3)_5$ .

Figure S3. Raman spectrum of solid  $\text{CH}_3\text{CN} \cdot \text{Ta}(\text{N}_3)_5$ .

Figure S4. IR and Raman spectra of  $[\text{PPh}_4][\text{Nb}(\text{N}_3)_6]$ .

Figure S5. IR and Raman spectra of  $[\text{PPh}_4][\text{Ta}(\text{N}_3)_6]$ .

Table S1. Comparison of observed and unscaled calculated vibrational frequencies [ $\text{cm}^{-1}$ ] and intensities for  $\text{Nb}(\text{N}_3)_5$ .

Table S2. Comparison of observed and unscaled calculated vibrational frequencies [ $\text{cm}^{-1}$ ] and intensities for  $\text{Ta}(\text{N}_3)_5$ .

Table S3. Comparison of observed and unscaled calculated vibrational frequencies [ $\text{cm}^{-1}$ ] and intensities for  $\text{CH}_3\text{CN} \cdot \text{Nb}(\text{N}_3)_5$ .

Table S4. Comparison of observed and unscaled calculated vibrational frequencies [ $\text{cm}^{-1}$ ] and intensities for  $\text{CH}_3\text{CN} \cdot \text{Ta}(\text{N}_3)_5$ .

Table S5. Comparison of observed and unscaled calculated vibrational frequencies [ $\text{cm}^{-1}$ ] and intensities for  $[\text{Ta}(\text{N}_3)_6]^-$ .

---

[\*] Dr. R. Haiges, Dr. T. Schroer, Dr. M. Yousufuddin, Prof. Dr. K. O. Christe  
 Loker Research Institute and Department of Chemistry  
 University of Southern California  
 Los Angeles, CA 90089-1661 (USA)  
 Fax: (+1) 213-740-6679  
 E-mail: [haiges@usc.edu](mailto:haiges@usc.edu), [kchriste@usc.edu](mailto:kchriste@usc.edu)  
 Dr. J. A. Boatz  
 Space and Missile Propulsion Division  
 Air Force Research Laboratory (AFRL/PRSP)

10 East Saturn Boulevard, Bldg 8451  
Edwards Air Force Base, CA 93524 (USA)

[\*\*] This work was funded by the Air Force Office of Scientific Research and the National Science Foundation. We thank Prof. Dr. G. A. Olah, and Dr. M. Berman, for their steady support, and Prof. D. Dixon, Prof. Dr. R. Bau, Drs. R. Wagner and W. W. Wilson, and C. Bigler Jones for their help and stimulating discussions. We gratefully acknowledge grants of computer time at the Aeronautical Systems Center (Wright-Patterson Air Force Base, Dayton, OH), the Naval Oceanographic Office (Stennis Space Center, MS), the Engineer Research and Development Center (Vicksburg, MS), the Army Research Laboratory (Aberdeen Proving Ground, MD), and the Army High Performance Computing Research Center (Minneapolis, MN), under sponsorship of the Department of Defense High Performance Computing Modernization Program Office.



Figure S1. IR and Raman spectrum of solid  $\text{Nb}(\text{N}_3)_5$ . The band marked by an asterisk (\*) is due to the Teflon-FEP sample tube.

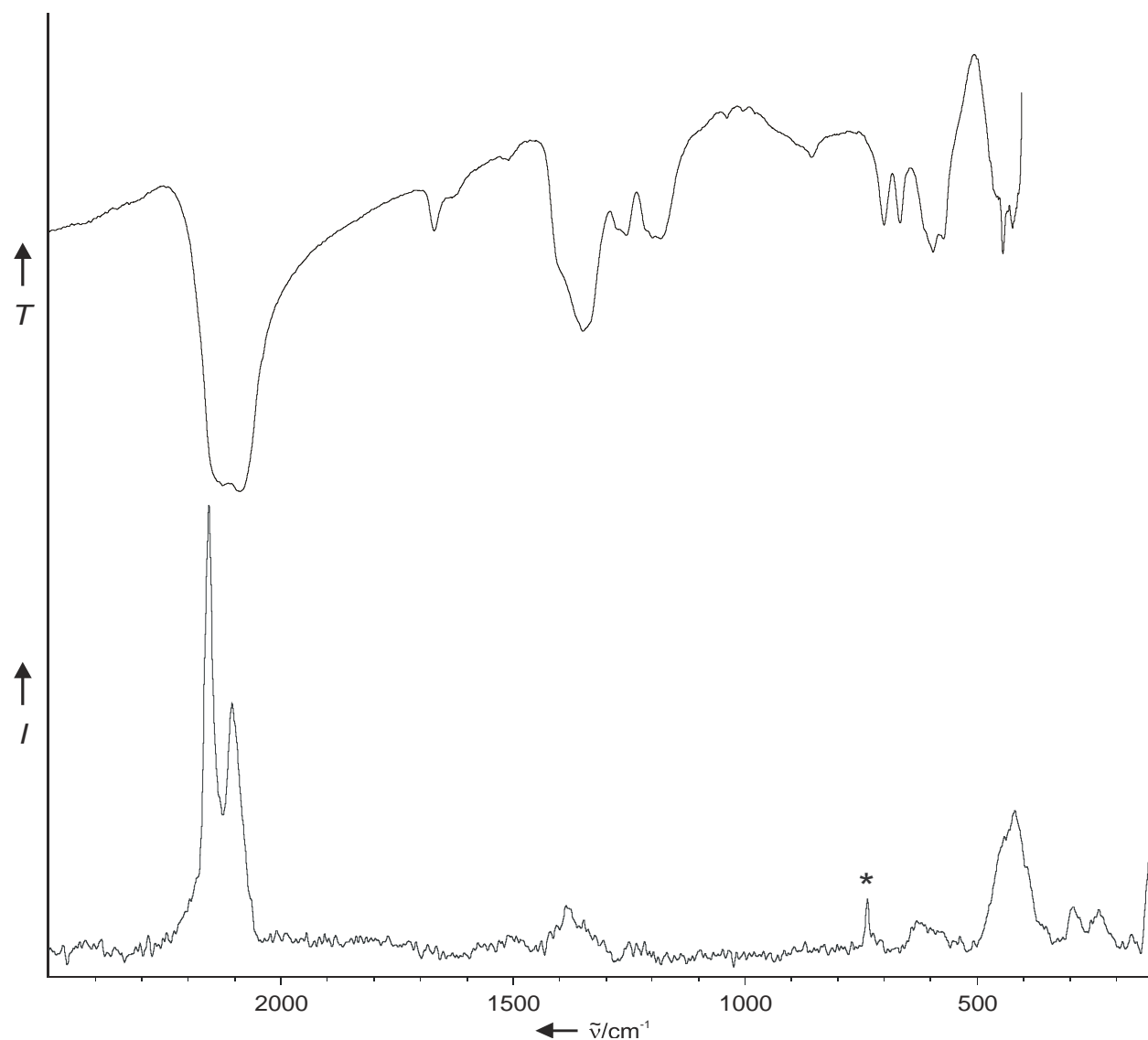


Figure S2. IR and Raman spectra of  $\text{Ta}(\text{N}_3)_5$ . The band marked by an asterisk (\*) is due to the Teflon-FEP sample tube.

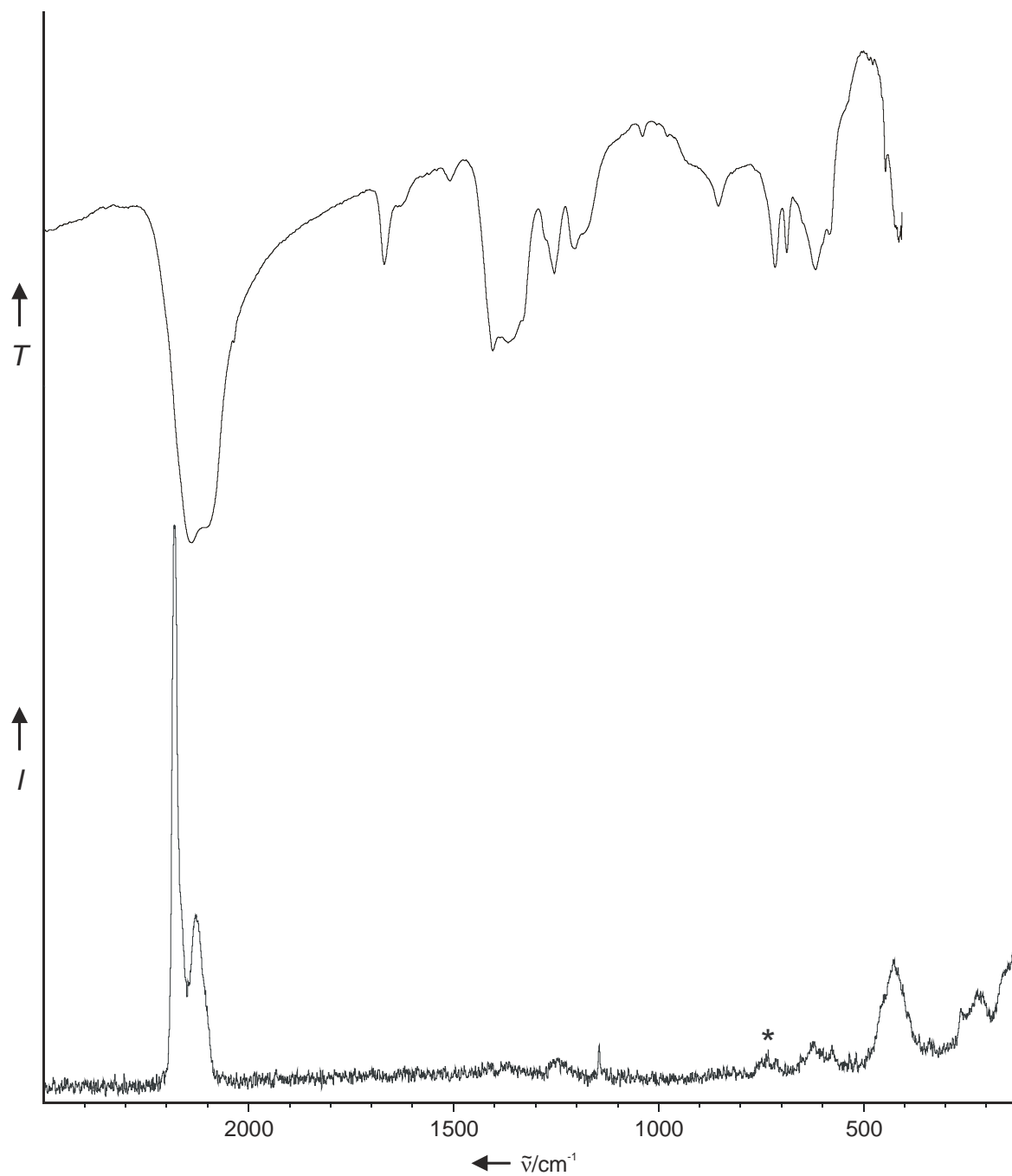


Figure S3. Raman spectrum of solid  $\text{CH}_3\text{CN}\cdot\text{Ta}(\text{N}_3)_5$ . The band marked by an asterisk (\*) is due to the Teflon-FEP sample tube.

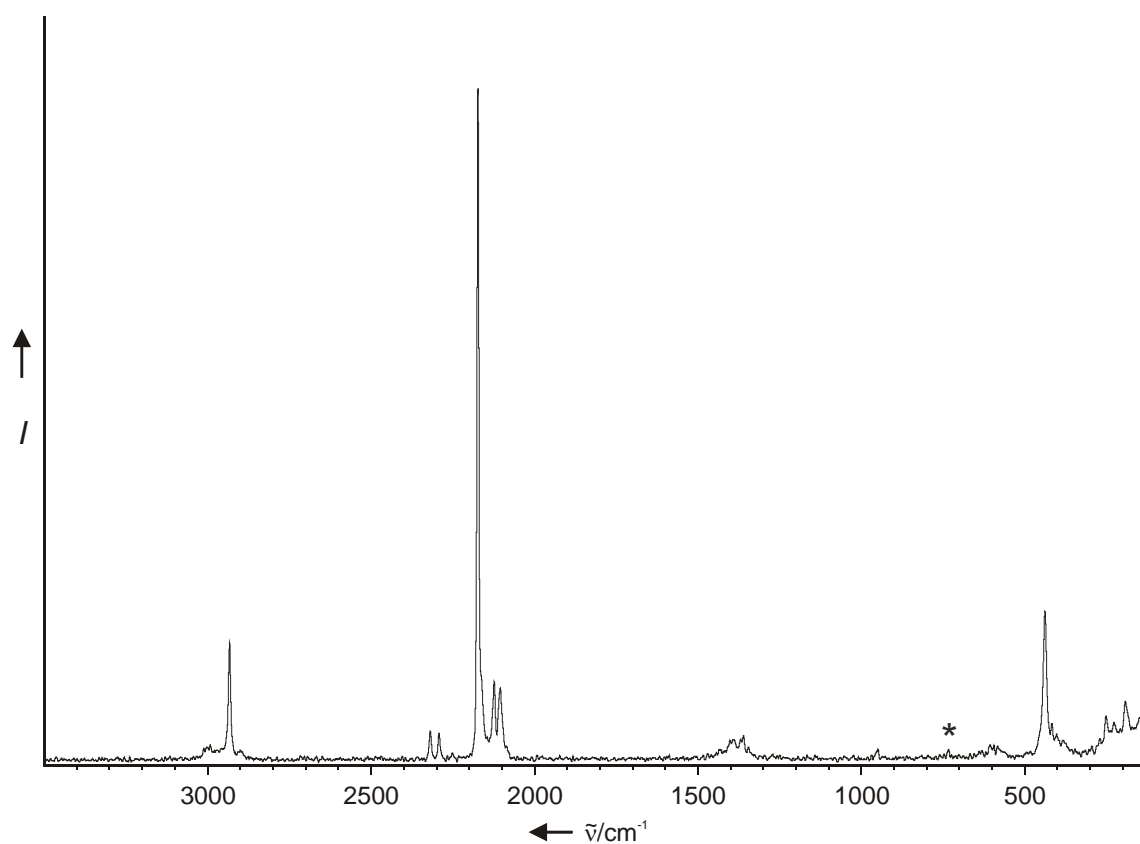


Figure S4. IR and Raman spectra of  $[\text{PPh}_4][\text{Nb}(\text{N}_3)_6]$ . The bands belonging to the  $[\text{Nb}(\text{N}_3)_6]^-$  ion are marked with a diamond ( $\blacklozenge$ ).

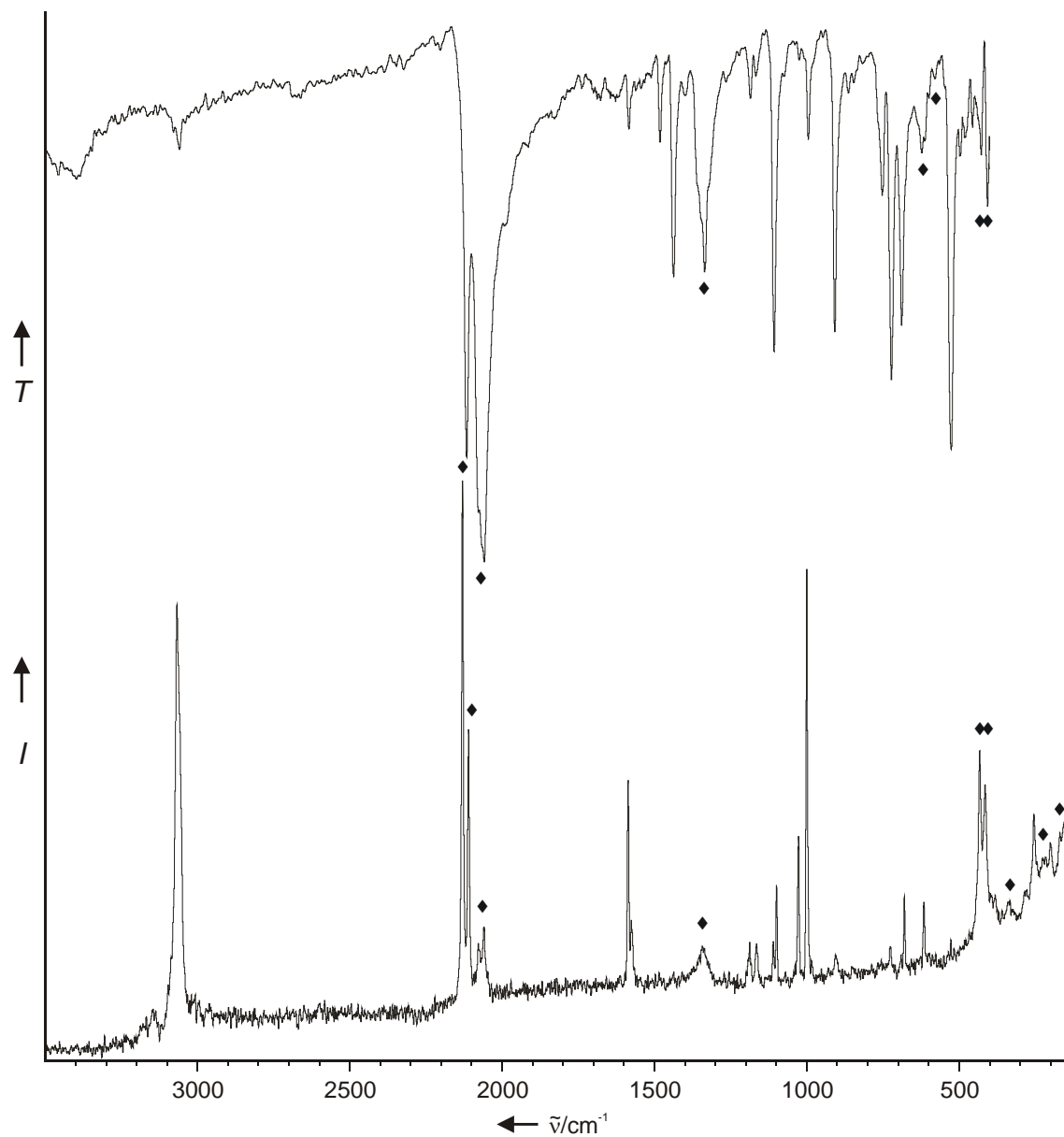


Figure S5. IR and Raman spectra of  $[\text{PPh}_4][\text{Ta}(\text{N}_3)_6]$ . The bands belonging to the  $[\text{Ta}(\text{N}_3)_6]^-$  ion are marked with a diamond ( $\blacklozenge$ ). The band marked by an asterisk (\*) is due to the Teflon-FEP sample tube.

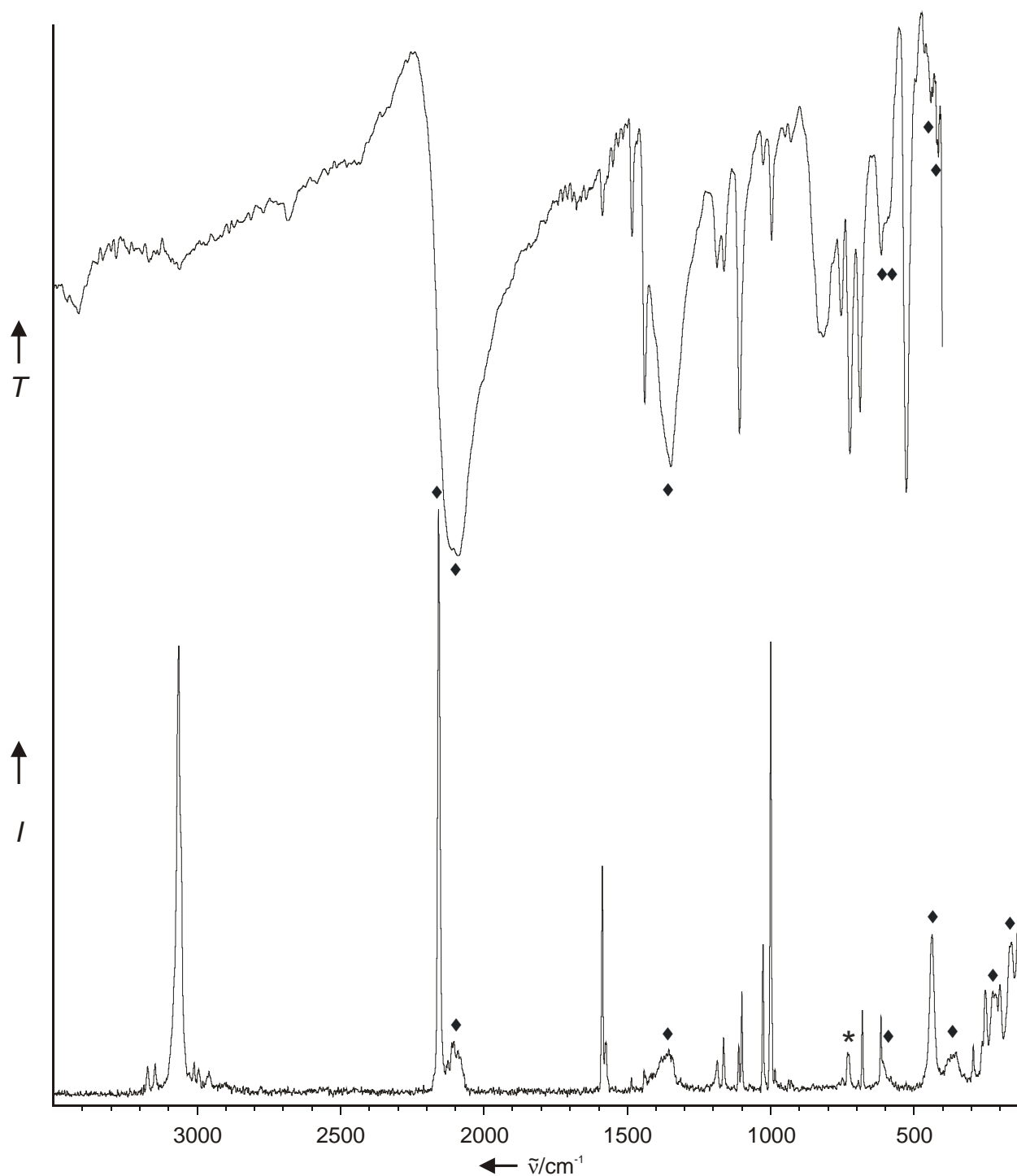


Table S1. Comparison of observed<sup>[a]</sup> and unscaled calculated vibrational frequencies [cm<sup>-1</sup>] and intensities<sup>[b]</sup> for Nb(N<sub>3</sub>)<sub>5</sub>

		observed		calculated (IR)[Raman]	
description		IR	Ra	B3LYP/SBK+(d)	MP2/SBK+(d)
v <sub>1</sub>	v <sub>as</sub> N <sub>3</sub>		2155 [10.0]	2235 (62) [1340]	2063 (806) [590]
v <sub>2</sub>	v <sub>as</sub> N <sub>3</sub>	2124 vs		2209 (2722) [241]	2074 (1918) [141]
v <sub>3</sub>	v <sub>as</sub> N <sub>3</sub>	2088 vs		2204 (1124) [250]	2061 (1261) [34]
v <sub>4</sub>	v <sub>as</sub> N <sub>3</sub>		2106 [5.5]	2200 (816) [306]	2059 (391) [246]
v <sub>5</sub>	v <sub>as</sub> N <sub>3</sub>			2179 (343) [210]	2044 (415) [28]
v <sub>6</sub>	v <sub>s</sub> N <sub>3</sub>		1385 [1.6]	1435 (172) [117]	1319 (36) [17]
v <sub>7</sub>	v <sub>s</sub> N <sub>3</sub>	1374 m		1403 (611) [31]	1312 (319) [16]
v <sub>8</sub>	v <sub>s</sub> N <sub>3</sub>			1375 (252) [8.4]	1294 (122) [20]
v <sub>9</sub>	v <sub>s</sub> N <sub>3</sub>	1347 s		1364 (453) [3.9]	1292 (206) [46]
v <sub>10</sub>	v <sub>s</sub> N <sub>3</sub>			1337 (350) [4.4]	1263 (111) [21]
v <sub>11</sub>	δN <sub>3</sub>			598 (5.6) [2.8]	596 (5.8) [10]
v <sub>12</sub>	δN <sub>3</sub>			587 (0.75) [5.8]	575 (83) [2.6]
v <sub>13</sub>	δN <sub>3</sub>		628 [0.7]	583 (57) [90]	567 (79) [3.4]
v <sub>14</sub>	δN <sub>3</sub>			580 (48) [2.5]	558 (115) [0.5]
v <sub>15</sub>	δN <sub>3</sub>		590 sh	580 (51) [0.22]	533 (3.6) [0.39]
v <sub>16</sub>	δN <sub>3</sub>	591 mw		579 (84) [6.6]	552 (39) [23]
v <sub>17</sub>	δN <sub>3</sub>			571 (9.7) [77]	521 (4.8) [1.6]
v <sub>18</sub>	δN <sub>3</sub>	569 w		567 (1.3) [2.1]	519 (6.5) [1.3]
v <sub>19</sub>	δN <sub>3</sub>			559 (4.2) [0.63]	506 (0.25) [2.3]
v <sub>20</sub>	δN <sub>3</sub>			552 (2.8) [1.2]	499 (6.4) [3.1]
v <sub>21</sub>	v <sub>as</sub> MN <sub>3</sub> eq	450 sh		472 (164) [5.0]	468 (159) [7.8]
v <sub>22</sub>	v <sub>as</sub> MN <sub>2</sub> ax	440 mw		463 (228) [2.9]	466 (247) [9.6]
v <sub>23</sub>	v <sub>as</sub> MN <sub>3</sub> eq	422 w	427 sh	444 (202) [14]	455 (301) [14]
v <sub>24</sub>	v <sub>s</sub> MN <sub>3</sub> eq		413 [3.2]	424 (100) [39]	416 (18) [238]
v <sub>25</sub>	v <sub>s</sub> MN <sub>2</sub> ax		360 sh	363 (0.63) [15]	372 (0.07) [42]
v <sub>26</sub>	δ <sub>umbrella</sub> MN <sub>3</sub>		288 [0.7]	285 (9.4) [29]	281 (8.8) [25]
v <sub>27</sub>	δ <sub>sciss</sub> MN <sub>3</sub>			266 (1.4) [6.3]	253 (0.37) [11]
v <sub>28</sub>	δ <sub>sciss</sub> MN <sub>3</sub>			243 (2.1) [16]	252 (1.2) [31]
v <sub>29</sub>	ρMN <sub>2</sub>			227 (0.21) [1.2]	212 (0.003) [5.6]
v <sub>30</sub>	ρMN <sub>2</sub>		234 [0.7]	208 (10) [36]	192 (8.6) [35]
v <sub>31</sub>	δ <sub>sciss</sub> MN <sub>2</sub>			143 (0.48) [13]	153 (0.36) [13]
v <sub>32</sub>	δ <sub>sciss</sub> MN <sub>2</sub>			134 (0.06) [1.9]	146 (0.11) [4.4]
v <sub>33</sub>	τ			103 (0.03) [6.5]	101 (0.11) [4.4]
v <sub>34</sub>	τ			100 (0.56) [7.2]	101 (1.9) [19]
v <sub>35</sub>	τ			90 (0.13) [0.99]	89 (0.13) [3.7]
v <sub>36</sub>	τ			57 (0.34) [15]	68 (0.33) [7.2]
v <sub>37</sub>	τ			53 (1.1) [6.3]	48 (1.1) [10]
v <sub>38</sub>	τ			45 (0.008) [13]	40 (0.05) [16]
v <sub>39</sub>	τ			43 (0.44) [23]	39 (0.17) [29]
v <sub>40</sub>	τ			41 (0.25) [20]	32 (0.012) [20]
v <sub>41</sub>	τ			29 (0.67) [16]	27 (0.44) [26]
v <sub>42</sub>	τ			18 (0.45) [1.7]	6 (0.61) [8.3]

[a] In addition to the bands listed in this table, the following weak infrared bands were observed which are attributed to overtones or combination bands: 1667 w, 1263 w, 1195 sh, 1176 w, 1037 vvw, 696 w, 660 w. [b] Calculated IR and Raman intensities are given in km mol<sup>-1</sup> and Å<sup>4</sup> amu<sup>-1</sup>.

Table S2. Comparison of observed<sup>[a]</sup> and unscaled calculated vibrational frequencies [cm<sup>-1</sup>] and intensities<sup>[b]</sup> for Ta(N<sub>3</sub>)<sub>5</sub>.

description		observed IR	Ra	calculated (infrared) [Raman] B3LYP/SBK+(d)	MP2/SBK+(d)
v <sub>1</sub>	v <sub>as</sub> N <sub>3</sub>		2182 [10.0]	2260 (43) [1109]	2134 (696) [316]
v <sub>2</sub>	v <sub>as</sub> N <sub>3</sub>	2141 vs		2233 (3271) [125]	2132 (2089) [139]
v <sub>3</sub>	v <sub>as</sub> N <sub>3</sub>		2129 [3.3]	2217 (895) [259]	2097 (823) [53]
v <sub>4</sub>	v <sub>as</sub> N <sub>3</sub>	2103 vs		2214 (1202) [170]	2086 (1230) [10]
v <sub>5</sub>	v <sub>as</sub> N <sub>3</sub>			2210 (319) [246]	2085 (673) [48]
v <sub>6</sub>	v <sub>s</sub> N <sub>3</sub>			1473 (7.2) [21]	1348 (29) [88]
v <sub>7</sub>	v <sub>s</sub> N <sub>3</sub>	1403 ms		1451 (857) [19]	1334 (368) [6.5]
v <sub>8</sub>	v <sub>s</sub> N <sub>3</sub>			1389 (15) [7.9]	1314 (124) [60]
v <sub>9</sub>	v <sub>s</sub> N <sub>3</sub>	1364 m		1375 (615) [5.7]	1303 (149) [34]
v <sub>10</sub>	v <sub>s</sub> N <sub>3</sub>			1370 (450) [10]	1299 (198) [51]
v <sub>11</sub>	δN <sub>3</sub>			600(2.0) [1.5]	566 (1.6) [0.61]
v <sub>12</sub>	δN <sub>3</sub>		623 [1.1]	599 (1.2) [15]	562 (0.98) [1.7]
v <sub>13</sub>	δN <sub>3</sub>	613 mw		586 (13) [0.34]	547 (54) [0.10]
v <sub>14</sub>	δN <sub>3</sub>			583 (19) [13]	545 (21) [10]
v <sub>15</sub>	δN <sub>3</sub>		590 sh	576 (2.7) [66]	550 (1.2) [24]
v <sub>16</sub>	δN <sub>3</sub>			572 (18) [0.59]	543 (0.59) [1.4]
v <sub>17</sub>	δN <sub>3</sub>			565 (37) [1.7]	538 (1.1) [0.12]
v <sub>18</sub>	δN <sub>3</sub>	578 w		563 (62) [9.8]	539 (18) [8.2]
v <sub>19</sub>	δN <sub>3</sub>			560 (9.9) [1.7]	530 (16) [0.08]
v <sub>20</sub>	δN <sub>3</sub>			552 (4.7) [3.1]	532 (27) [0.42]
v <sub>21</sub>	v <sub>as</sub> MN <sub>3</sub> eq		450 sh	444 (137) [6.5]	443 (188) [4.0]
v <sub>22</sub>	v <sub>as</sub> MN <sub>2</sub> ax			442 (149) [1.4]	445 (167) [1.7]
v <sub>23</sub>	v <sub>as</sub> MN <sub>3</sub> eq		426 [2.5]	439 (29) [38]	431 (4.3) [172]
v <sub>24</sub>	v <sub>s</sub> MN <sub>3</sub> eq	410 mw		388 (265) [9.1]	391 (349) [7.1]
v <sub>25</sub>	v <sub>s</sub> MN <sub>2</sub> ax		390 sh	360 (12) [47]	359 (2.9) [53]
v <sub>26</sub>	δ <sub>umbrella</sub> MN <sub>3</sub>			288 (10) [3.2]	282 (11) [4.1]
v <sub>27</sub>	δ <sub>sciss</sub> MN <sub>3</sub>			268 (9.8) [10]	255 (20) [5.9]
v <sub>28</sub>	δ <sub>sciss</sub> MN <sub>3</sub>		256 [1.7]	258 (5.5) [63]	259 (1.6) [16]
v <sub>29</sub>	ρMN <sub>2</sub>			253 (3.7) [0.23]	238 (7.5) [0.08]
v <sub>30</sub>	ρMN <sub>2</sub>		221 [2.0]	207 (22) [21]	189 (22) [4.6]
v <sub>31</sub>	δ <sub>sciss</sub> MN <sub>2</sub>			150 (0.18) [5.0]	149 (0.85) [8.9]
v <sub>32</sub>	δ <sub>sciss</sub> MN <sub>2</sub>			123 (1.5) [160]	141 (1.5) [11]
v <sub>33</sub>	τ			109 (0) [3.6]	115 (0.006) [2.4]
v <sub>34</sub>	τ			101 (0.10) [8.4]	94 (0.11) [13]
v <sub>35</sub>	τ			100 (0.11) [11]	93 (0.07) [23]
v <sub>36</sub>	τ			48 (1.0) [2.6]	42 (0.62) [6.7]
v <sub>37</sub>	τ			47 (0.002) [13]	44 (0.07) [11]
v <sub>38</sub>	τ			40 (0.36) [47]	35 (0.29) [28]
v <sub>39</sub>	τ			40 (0.11) [21]	33 (0.19) [15]
v <sub>40</sub>	τ			39 (0.13) [17]	35 (0.005) [24]
v <sub>41</sub>	τ			21 (0.65) [0.65]	12 (0.80) [0.73]
v <sub>42</sub>	τ			17 (0.70) [3.4]	9 (0.91) [2.2]

[a] In addition to the bands listed in this table, the following weak infrared bands were observed which are attributed to overtones or combination bands: 1669 w, 1508 vw, 1274 sh, 1252 w, 1203 w, 1180 sh, 1036 vw, 850 w, 712 w, 683 w. [b] Calculated IR and Raman intensities are given in km mol<sup>-1</sup> and Å<sup>4</sup> amu<sup>-1</sup>.

Table S3. Comparison of observed and unscaled calculated<sup>[a]</sup> vibrational frequencies [cm<sup>-1</sup>] and intensities for CH<sub>3</sub>CN·Nb(N<sub>3</sub>)<sub>5</sub>.

description		observed Ra	calculated (infrared) [Raman] B3LYP/SBK+(d) MP2/SBK+(d)	
v <sub>1</sub>	v <sub>s</sub> CH <sub>3</sub>	2928 (1.8)	3111 (1.1) [54]	3180 (1.8) [32]
v <sub>2</sub>	v <sub>as</sub> CH <sub>3</sub>		3110 (1.2) [52]	3179 (1.7) [56]
v <sub>3</sub>	v <sub>as</sub> CH <sub>3</sub>		3005 (0.82) [192]	3051 (0.83) [173]
v <sub>4</sub>	vCN	2315 (1.2) 2289 (1.1)	2378 (75) [138]	2218 (22) [62]
v <sub>5</sub>	v <sub>as</sub> N <sub>3</sub>	2140 (10.0)	2238 (751) [1019]	2168 (624) [67]
v <sub>6</sub>	v <sub>as</sub> N <sub>3</sub>	2121 (1.5)	2202 (1935) [364]	2131 (770) [16]
v <sub>7</sub>	v <sub>as</sub> N <sub>3</sub>	2097 (1.9)	2176 (1528) [163]	2129 (514) [45]
v <sub>8</sub>	v <sub>as</sub> N <sub>3</sub>	2090 (1.6)	2176 (1527) [163]	2102 (732) [609]
v <sub>9</sub>	v <sub>as</sub> N <sub>3</sub>	2074 (2.2) 2058 (1.4)	2153 (0.11) [205]	2100 (1690) [88]
v <sub>10</sub>	v <sub>s</sub> N <sub>3</sub>		1473 (470) [12]	1460 (17) [8.7]
v <sub>11</sub>	δ <sub>sciss</sub> CH <sub>3</sub>	1415 (1.3)	1434 (14) [7.7]	1460 (11) [4.7]
v <sub>12</sub>	δ <sub>sciss</sub> CH <sub>3</sub>		1434 (14) [7.6]	1404 (6.6) [8.7]
v <sub>13</sub>	v <sub>s</sub> N <sub>3</sub>	1351 (1.1)	1413 (246) [4.3]	1345 (252) [35]
v <sub>14</sub>	v <sub>s</sub> N <sub>3</sub>	1331 (1.1)	1394 (374) [2.2]	1294 (29) [22]
v <sub>15</sub>	v <sub>s</sub> N <sub>3</sub>		1394 (379) [2.3]	1288 (160) [11]
v <sub>16</sub>	v <sub>s</sub> N <sub>3</sub>		1391 (6.5) [4.0]	1276 (35) [22]
v <sub>17</sub>	δ <sub>s</sub> CH <sub>3</sub>	1363 (1.2)	1375 (4.9) [16]	1274 (130) [16]
v <sub>18</sub>	δ <sub>rock</sub> CH <sub>3</sub>		1046 (0.78) [0.10]	1068 (0.42) [0.67]
v <sub>19</sub>	δ <sub>wag</sub> CH <sub>3</sub>		1046 (0.82) [0.10]	1066 (1.4) [0.69]
v <sub>20</sub>	vCC	947 (1.0)	934 (8.0) [5.6]	954 (12) [2.7]
v <sub>21</sub>	δN <sub>3</sub>	620 (1.2)	609 (5.4) [1.7]	612 (14) [15]
v <sub>22</sub>	δN <sub>3</sub>	610 (1.0)	598 (63) [2.9]	595 (22) [11]
v <sub>23</sub>	δN <sub>3</sub>		598 (63) [2.9]	594 (111) [8.5]
v <sub>24</sub>	δN <sub>3</sub>	599 (1.2)	594 (0.61) [0.12]	583 (92) [12]
v <sub>25</sub>	δN <sub>3</sub>	580 (1.1)	573 (0.006) [0.05]	519 (3.1) [0.31]
v <sub>26</sub>	δN <sub>3</sub>	566 (1.0)	565 (19) [0.50]	516 (0.46) [0.69]
v <sub>27</sub>	δN <sub>3</sub>		565 (20) [0.53]	511 (1.5) [4.9]
v <sub>28</sub>	δN <sub>3</sub>		564 (1.1) [0.03]	509 (6.2) [2.5]
v <sub>29</sub>	δN <sub>3</sub>	557 (1.1)	557 (12) [1.0]	495 (3.2) [0.88]
v <sub>30</sub>	δN <sub>3</sub>		557 (12) [1.0]	487 (15) [0.44]
v <sub>31</sub>	δN-C-C		456 (21) [0.12]	461 (233) [27]
v <sub>32</sub>	δN-C-C		456 (22) [0.12]	454 (261) [1.1]
v <sub>33</sub>	vNbN <sub>ax</sub>	441 (3.1)	444 (224) [31]	451 (272) [17]
v <sub>34</sub>	v <sub>as</sub> NbN <sub>4</sub>	435 (2.8)	427 (278) [1.5]	429 (14) [4.0]
v <sub>35</sub>	v <sub>as</sub> NbN <sub>4</sub>	423 (1.7)	427 (277) [1.5]	428 (20) [81]
v <sub>36</sub>	v <sub>sym</sub> NbN <sub>4 i p</sub>	419 (1.7)	411 (0.025) [87]	418 (20) [174]
v <sub>37</sub>	v <sub>sym</sub> NbN <sub>4 oo p</sub>	411 (2.0)	352 (0) [3.6]	372 (6.1) [2.9]
v <sub>38</sub>	vNbN <sub>CH<sub>3</sub>CN</sub>	281 (1.1)	296 (0.06) [1.4]	294 (14) [1.5]
v <sub>39</sub>	δ <sub>as</sub> NbN <sub>4</sub>	266 (1.3)	278 (17) [0.63]	265 (8.8) [1.2]
v <sub>40</sub>	δ <sub>as</sub> NbN <sub>4</sub>	256 (1.3)	278 (17) [0.63]	262 (15) [15]
v <sub>41</sub>	δNbN <sub>5</sub>	248 (1.4)	255 (0.02) [23]	247 (0.50) [15]
v <sub>42</sub>	δNbN <sub>5</sub>	226 (1.6)	221 (0.64) [2.1]	232 (1.2) [19]
v <sub>43</sub>	δNbN <sub>5</sub>		221 (0.66) [2.1]	224 (2.2) [1.7]
v <sub>44</sub>	δCH <sub>3</sub> CN-NbN <sub>5</sub>		203 (0.10) [0.34]	202 (4.8) [6.5]
v <sub>45</sub>	δCH <sub>3</sub> CN-NbN <sub>5</sub>		203 (0.09) [0.36]	190 (0.01) [2.7]
v <sub>46</sub>	δNbN <sub>5</sub>	189 (1.3)	200 (0.09) [2.7]	182 (0.96) [12]
v <sub>47</sub>	δNbN <sub>5</sub>	180 (1.3)	183 (0) [16]	164 (0.01) [4.3]
v <sub>48</sub>	τ	139 (1.6)	119 (0.70) [6.6]	117 (0.28) [14]
v <sub>49</sub>	τ	96 (2.9)	118 (0.68) [6.6]	115 (1.1) [13]
v <sub>50</sub>	τ		83 (0) [0]	64 (2.7) [16]
v <sub>51</sub>	τ		52 (3.3) [31]	62 (0.05) [0.81]
v <sub>52</sub>	τ		48 (0.004) [24]	59 (0.11) [9.1]
v <sub>53</sub>	τ		38 (0.009) [16]	55 (1.7) [31]
v <sub>54</sub>	τ		34 (2.1) [1.7]	48 (0.48) [1.9]
v <sub>55</sub>	τ		34 (2.0) [1.9]	39 (1.5) [7.3]
v <sub>56</sub>	τ		29 (1.6) [3.4]	31 (1.9) [3.7]
v <sub>57</sub>	τ		28 (1.7) [3.3]	26 (0.49) [16]



$\nu_{58}$	$\tau$	12 (0.11) [145]	25 (0.89) [16]
$\nu_{59}$	$\tau$	9 (0.11) [15]	20 (0.55) [13]
$\nu_{60}$	unhindered CH <sub>3</sub> $\tau$	13i (0.04) [0.01]	16 (0.008) [19]

---

[a] Calculated IR and Raman intensities are given in  $\text{km mol}^{-1}$  and  $\text{\AA}^4 \text{amu}^{-1}$ , respectively. The given assignments of the observed frequencies are for the calculated B3LYP frequencies. The MP2 values have not been matched with either the B3LYP values or the observed spectrum.

Table S4. Comparison of observed and unscaled calculated<sup>[a]</sup> vibrational frequencies [cm<sup>-1</sup>] and intensities for CH<sub>3</sub>CN·Ta(N<sub>3</sub>)<sub>5</sub>.

description		observed Ra	calculated (infrared) [Raman] B3LYP/SBK+(d)	MP2/SBK+(d)
v <sub>1</sub>	v <sub>s</sub> CH <sub>3</sub>		3109 (1.3) [56]	3181 (1.6) [46]
v <sub>2</sub>	v <sub>as</sub> CH <sub>3</sub>		3109 (1.3) [55]	3179 (2.0) [40]
v <sub>3</sub>	v <sub>as</sub> CH <sub>3</sub>	2933 [1.7]	3004 (0.96) [202]	3051 (0.71) [166]
v <sub>4</sub>	vCN	2319 [0.5]	2383 (74) [166]	2235 (23) [79]
v <sub>5</sub>	vCN	2291 [0.5]	2222(2045) [360]	2168 (1157) [5.2]
v <sub>6</sub>	v <sub>as</sub> N <sub>3</sub>	2172 [10.0]	2260 (655) [1025]	2154 (128) [363]
v <sub>7</sub>	v <sub>as</sub> N <sub>3</sub>	2162 [1.2]	2195 (1739) [125]	2167 (1155) [4.6]
v <sub>8</sub>	v <sub>as</sub> N <sub>3</sub>	2123 [1.2]	2195 (1735) [125]	2168 (1157) [5.2]
v <sub>9</sub>	v <sub>as</sub> N <sub>3</sub>	2103 [1.1]	2173 (0.007) [181]	2137 (2378) [92]
v <sub>10</sub>	v <sub>s</sub> N <sub>3</sub>		1487 (428) [28]	1462 (13) [7.1]
v <sub>11</sub>	δ <sub>sciss</sub> CH <sub>3</sub>	1389 [0.4]	1434 (15) [8.2]	1460 (15) [7.1]
v <sub>12</sub>	δ <sub>sciss</sub> CH <sub>3</sub>		1433 (15) [8.4]	1404 (4.1) [9.2]
v <sub>13</sub>	v <sub>s</sub> N <sub>3</sub>		1432 (264) [29]	1364 (260) [69]
v <sub>14</sub>	v <sub>s</sub> N <sub>3</sub>		1410 (417) [6.8]	1318 (59) [42]
v <sub>15</sub>	v <sub>s</sub> N <sub>3</sub>		1410 (418) [6.9]	1307 (110) [48]
v <sub>16</sub>	v <sub>s</sub> N <sub>3</sub>		1409 (0.08)[12]	1301 (181) [27]
v <sub>17</sub>	δ <sub>s</sub> CH <sub>3</sub>	1361 [0.4]	1374 (3.7) [16]	1298 (89) [44]
v <sub>18</sub>	δ <sub>rock</sub> CH <sub>3</sub>		1046 (0.91) [0.055]	1067 ( 0.41) [0.33]
v <sub>19</sub>	δ <sub>wag</sub> CH <sub>3</sub>		1046 (0.93) [0.082]	1067 (0.4) [0.33]
v <sub>20</sub>	vCC	948 [0.3]	935 (7.5) [15]	958 (12) [3.5]
v <sub>21</sub>	δN <sub>3</sub>		608 (5.7) [1.2]	592 (2.1) [11]
v <sub>22</sub>	δN <sub>3</sub>		596 (29) [1.7]	572 (50) [7.1]
v <sub>23</sub>	δN <sub>3</sub>		596 (28) [1.7]	576 (4.0) [7.3]
v <sub>24</sub>	δN <sub>3</sub>	592 [0.3]	593 (0.09) ) [28]	572 (46) ) [6.6]
v <sub>25</sub>	δN <sub>3</sub>		585 (0.03) [0]	535 (12) [0.37]
v <sub>26</sub>	δN <sub>3</sub>		584 (1.5) [0.06]	529 (0.10) [0.35]
v <sub>27</sub>	δN <sub>3</sub>		584 (41) [0.28]	534 (12) [0.30]
v <sub>28</sub>	δN <sub>3</sub>		584 (43) [0.26]	529 (1.6) [0.06]
v <sub>29</sub>	δN <sub>3</sub>		578 (0.11) [1.6]	523 (3.8) [0.28]
v <sub>30</sub>	δN <sub>3</sub>		578 (0.19) [1.6]	523 (2.8) [0.32]
v <sub>31</sub>	δN-C-C		471 (1.8) [0.82]	439 (7.1) [0.05]
v <sub>32</sub>	δN-C-C		471 (1.9) [0.82]	440 (16) [23]
v <sub>33</sub>	vNbN <sub>ax</sub>	438 [2.1]	424 (0.53) [83]	433 (21) [69]
v <sub>34</sub>	v <sub>as</sub> NbN <sub>4</sub>	417 [0.6]	410 (170) [20]	413 (188) [100]
v <sub>35</sub>	v <sub>as</sub> NbN <sub>4</sub>		398 (242) [0.27]	411 (268) [3.0]
v <sub>36</sub>	v <sub>sym</sub> NbN <sub>4</sub> i p		398 (242) [0.26]	412 (272) [0.67]
v <sub>37</sub>	v <sub>sym</sub> NbN <sub>4</sub> oo p		366 (0) [1.3]	382 (0.32) [3.1]
v <sub>38</sub>	vNbNCH <sub>3</sub> CN		303 (0) [2.1]	297 (0.06) [0.37]
v <sub>39</sub>	δ <sub>as</sub> NbN <sub>4</sub>		274 (33) [0.32]	253 (38) [2.0]
v <sub>40</sub>	δ <sub>as</sub> NbN <sub>4</sub>		273 (32) [0.31]	253 (40) [1.9]
v <sub>41</sub>	δNbN <sub>5</sub>	250 [0.7]	246 (3.5) [24]	236 (0.87) [0.83]
v <sub>42</sub>	δNbN <sub>5</sub>	226 [0.6]	226 (0.43) [0.98]	228 (1.8) [30]
v <sub>43</sub>	δNbN <sub>5</sub>		226 (0.43) [0.98]	215 (11) [1.2]
v <sub>44</sub>	δCH <sub>3</sub> CN-NbN <sub>5</sub>		210 (0.32) [0.12]	215 (10) [1.4]
v <sub>45</sub>	δCH <sub>3</sub> CN-NbN <sub>5</sub>		210 (0.32) [0.11]	183 (0.96) [0.79]
v <sub>46</sub>	δNbN <sub>5</sub>		203 (1.2) [0.27]	182 (0.97) [0.83]
v <sub>47</sub>	δNbN <sub>5</sub>	192 [0.9]	182 (0.0004) [15]	169 (0) [14]
v <sub>48</sub>	τ		126 (0) [0]	107 (2.6) [11]
v <sub>49</sub>	τ		115 (0.95) [6.0]	107 (2.4) [11]
v <sub>50</sub>	τ		115 (0.96) [6.0]	86 (0.005) [0.006]
v <sub>51</sub>	τ		57 (0.0004) [24]	45 (0.027) [24]
v <sub>52</sub>	τ		48 (3.7) [28]	42 (4.1) [33]
v <sub>53</sub>	τ		40 (2.0) [0.12]	34 (1.1) [2.2]
v <sub>54</sub>	τ		40 (2.1) [0.13]	37 (1.2) [2.6]
v <sub>55</sub>	τ		33 (1.0) [6.7]	30 (0.0025) [11]
v <sub>56</sub>	τ		33 (0.99) [6.7]	17 (0.78) [17]
v <sub>57</sub>	τ		30 (0.003) [15]	27 (0.019) [12]
v <sub>58</sub>	τ		26 (0.82) [11]	17 (0.34) [16]

$\nu_{59}$	$\tau$	26 (0.77) [11]	15 (0.40) [0.72]
$\nu_{60}$	$\tau$	10 (0.0004) [0.019]	7 (0.66) [0.44]

[a] Calculated IR and Raman intensities are given in  $\text{km mol}^{-1}$  and  $\text{\AA}^4 \text{amu}^{-1}$ , respectively. The given assignments of the observed frequencies are for the calculated B3LYP frequencies. The MP2 values have not been matched with either the B3LYP values or the observed spectrum.

Table S5. Comparison of observed and unscaled calculated vibrational frequencies [ $\text{cm}^{-1}$ ] and intensities for  $[\text{Ta}(\text{N}_3)_6]^{-[\text{a}]}$  in point group  $\text{C}_1$

		observed		Calculated (IR) [Raman]	
	description	IR	Ra	B3LYP/SBK+(d)	MP2/SBK+(d)
V <sub>1</sub>	$\nu_{\text{as}}\text{N}_3$		2159 [10.0]	2238 (100) [940]	2281 (1924) [5.1]
V <sub>2</sub>	$\nu_{\text{as}}\text{N}_3$	2124 vs	2111 [1.0]	2199 (2670) [120]	2181 (1926) [5.1]
V <sub>3</sub>	$\nu_{\text{as}}\text{N}_3$	2113 vs	2103 [1.0]	2193 (2307) [130]	2168 (534) [0.86]
V <sub>4</sub>	$\nu_{\text{as}}\text{N}_3$	2096 vs	2091 [0.8]	2189 (3036) [38]	2169 (771) [0.59]
V <sub>5</sub>	$\nu_{\text{as}}\text{N}_3$	2087 vs	2081 [0.7]	2178 (8.1) [221]	2169 (59) [1.5]
V <sub>6</sub>	$\nu_{\text{as}}\text{N}_3$			2172 (176) [193]	2167 (0.021) [444]
V <sub>7</sub>	$\nu_{\text{s}}\text{N}_3$			1441 (14) [55]	1304 (0.0004) [123]
V <sub>8</sub>	$\nu_{\text{s}}\text{N}_3$	1383 m		1421 (197) [25]	1297 (7.1) [103]
V <sub>9</sub>	$\nu_{\text{s}}\text{N}_3$	1372 m		1417 (118) [28]	1298 (6.9) [103]
V <sub>10</sub>	$\nu_{\text{s}}\text{N}_3$	1360 ms	1355 [0.8]	1414 (336) [18]	1293 (157) [0.003]
V <sub>11</sub>	$\nu_{\text{t}}\text{N}_3$	1348 s		1412 (420) [7.7]	1292 (232) [67]
V <sub>12</sub>	$\nu_{\text{s}}\text{N}_3$			1409 (338) [13]	1292 (232) [67]
V <sub>13</sub>	$\delta\text{N}_3$	648 vw		605 (7.4) [0.49]	581 (0.0004) [8.6]
V <sub>14</sub>	$\delta\text{N}_3$	615 m	609 [0.6]	599 (30) [1.2]	563 (13) [4.7]
V <sub>15</sub>	$\delta\text{N}_3$	600 mw		597 (25) [1.6]	563 (12) [4.7]
V <sub>16</sub>	$\delta\text{N}_3$			595 (15) [1.9]	553 (23) [8.0]
V <sub>17</sub>	$\delta\text{N}_3$			594 (0.45) [0.60]	553 (23) [8.0]
V <sub>18</sub>	$\delta\text{N}_3$			592 (10) [0.54]	551 (20) [0.014]
V <sub>19</sub>	$\delta\text{N}_3$			590 (12) [1.4]	534 (0.04) [0.027]
V <sub>20</sub>	$\delta\text{N}_3$			586 (3.4) [0.35]	535 (0) [2.6]
V <sub>21</sub>	$\delta\text{N}_3$	585 mw		585 (16) [0.39]	534 (0.04) [0.029]
V <sub>22</sub>	$\delta\text{N}_3$			584 (20) [0.44]	530 (0.060) [1.1]
V <sub>23</sub>	$\delta\text{N}_3$		582 [0.4]	583 (16) [1.9]	530 (0.063) [1.1]
V <sub>24</sub>	$\delta\text{N}_3$	576 w		578 (17) [0.24]	521 (23) [0]
V <sub>25</sub>	$\nu\text{MN}$	433 w	437 [2.8]	418 (1.9) [73]	414 (0.0009) [155]
V <sub>26</sub>	$\nu\text{MN}$	418 mw		377 (281) [1.3]	389 (294) [0.10]
V <sub>27</sub>	$\nu\text{MN}$	414 mw	372 [0.7]	375 (288) [1.3]	389 (294) [0.10]
V <sub>28</sub>	$\nu\text{MN}$		364 [0.8]	369 (306) [0.63]	369 (357) [0]
V <sub>29</sub>	$\nu\text{MN}$		353 [0.8]	344 (7.4) [1.5]	341 (40) [5.2]
V <sub>30</sub>	$\nu\text{MN}$			337 (41) [2.1]	341 (40) [5.1]
V <sub>31</sub>	$\delta\text{MN}$			271 (31) [3.2]	266 (57) [4.8]
V <sub>32</sub>	$\delta\text{MN}$			261 (31) [2.7]	266 (57) [4.8]
V <sub>33</sub>	$\delta\text{MN}$			254 (9.6) [6.3]	256 (0) [27]
V <sub>34</sub>	$\delta\text{MN}$		225 [1.8]	233 (24) [13]	215 (4.5) [4.7]
V <sub>35</sub>	$\delta\text{MN}$			228 (17) [11]	215 (4.5) [4.7]
V <sub>36</sub>	$\delta\text{MN}$		215 [1.8]	221 (9.6) [7.4]	209 (40) [0]
V <sub>37</sub>	$\delta\text{MN}$		168 [2.6]	181 (0.76) [18]	167 (0) [19]
V <sub>38</sub>	$\delta\text{MN}$			176 (0.06) [7.5]	161 (0.28) [19]
V <sub>39</sub>	$\delta\text{MN}$		160 [2.6]	172 (0.34) [14]	161 (0.28) [19]
V <sub>40</sub>	$\tau$			91 (0.55) [7.3]	79 (3.6) [0]
V <sub>41</sub>	$\tau$			83 (0.13) [10]	44 (0.006) [19]
V <sub>42</sub>	$\tau$			79 (0.48) [0.69]	44 (0.004) [19]
V <sub>43</sub>	$\tau$			44 (2.4) [19]	43 (0) [28]
V <sub>44</sub>	$\tau$			41 (0.81) [18]	37 (1.7) [16]
V <sub>45</sub>	$\tau$			39 (1.2) [18]	37 (1.8) [16]
V <sub>46</sub>	$\tau$			38 (0.47) [17]	28 (0.73) [28]
V <sub>47</sub>	$\tau$			36 (2.8) [11]	28 (0.75) [28]
V <sub>48</sub>	$\tau$			35 (1.4) [7.3]	27 (0.0004) [3.6]
V <sub>49</sub>	$\tau$			30 (0.44) [3.9]	14 (0.60) [6.5]
V <sub>50</sub>	$\tau$			27 (0.22) [10]	14 (0.58) [6.3]
V <sub>51</sub>	$\tau$			22 (0.81) [6.5]	9 (2.8) [0.002]

[a] Calculated IR and Raman intensities are given in  $\text{km mol}^{-1}$  and  $\text{\AA}^4 \text{amu}^{-1}$ , respectively; observed spectra are for the solid  $[\text{P}(\text{C}_6\text{H}_5)_4]^+$  salt. The MP2 values have not been matched with either the B3LYP values or the observed spectrum.